

The Role of Formin-2 in the Development of Retinotectal Connectivity in *Danio rerio*

A Thesis

submitted to

Indian Institute of Science Education and Research Pune in partial fulfilment of the
requirements for the BS-MS Dual Degree Programme

by

Jayapriya C S



Indian Institute of Science Education and Research Pune

Dr. Homi Bhabha Road,
Pashan, Pune 411008, INDIA.

April, 2020

Supervisor: Dr. Aurnab Ghose

Your Name: Jayapriya C S

All rights reserved

Certificate

This is to certify that this dissertation entitled "**The Role of Formin-2 in the Development of retinotectal connectivity in *Danio rerio*.**" towards the partial fulfilment of the BS-MS dual degree programme at the Indian Institute of Science Education and Research, Pune represents study/work carried out by Jayapriya C S at Indian Institute of Science Education and Research under the supervision of Dr. Aurnab Ghose, Professor, Department of Biology, during the academic year 2019-2020.



Dr. Aurnab Ghose

Committee:

Dr. Aurnab Ghose

Dr. Nixon Abraham

This thesis is dedicated to

My Family

DECLARATION

I hereby declare that the matter embodied in the report entitled “The Role of Formin-2 in the development of retinotectal connectivity in *Danio rerio*.” are the results of the work carried out by me at the Department of Biology, Indian Institute of Science Education and Research, Pune, under the supervision of Dr.Aurnab Ghose and the same has not been submitted elsewhere for any other degree



Jayapriya C S

22/03/2020

ACKNOWLEDGEMENT

First and foremost, I would like to express my sincere gratitude to Dr. Aurnab Ghose for giving me the opportunity to work with him. His consistent support and guidance help me to improve myself. I would like to extend my gratitude to Dr. Nixon Abraham, a member of my thesis advisory committee for his guidance and discussion throughout the project. I would also like to thank Dhriti Nagar for her useful comments, remarks and engagement through the learning process of this master thesis. I would like to acknowledge Vijay Vittal and Rahul from the microscope facilities for teaching me to work with the microscope. I would also like to thank all my past and present lab members, especially Dhriti Nagar, Aditi Maduskar and Lisas Sewatkar for being there for me throughout the master thesis. I would like to extend my gratitude to my friends and my amazing roommate, Aditi Agarwal for their support and love. Last but not the least, I would love to thank my family: my mother, father, brother and sister for their support and care.

TABLE OF CONTENTS

Abstract	9
CHAPTER 1: INTRODUCTION	
1.1. Neural Circuit Development	10
1.2. Stages of neural circuit development	11
1.2.1. Cytoskeletal Remodelling in the Neural Circuitry	13
1.2.2. Formin-2	15
1.3. Zebrafish as a model organism	16
1.4. The retinotectal projection	17
1.4.1. Central projections of RGCs	19
1.4.2. Optic Tectum	20
1.5. Zebrafish innate visual behaviours	22
1.6. Motivation	23
CHAPTER 2: MATERIALS AND METHODS	24
2.1. Zebrafish Handling	
2.1.1. Transgenic lines	
2.1.1.1. <i>Tg(Brn3c:GAP43-GFP)</i>	
2.1.1.2. <i>Tg(Elavl3:GCamp6f)</i>	
2.2. Embryo microinjection -Morpholino Injection	24
2.3. Live Imaging	25
2.4. Whole-mount immunostaining	25
2.5. Imaging	26
2.6. Behaviour Assay	26
2.7. Calcium Imaging	27
2.8. Analysis	27
2.8.1. Live imaging	
2.8.2. Whole-mount immunostaining	
2.8.3. Behaviour Assay	

2.8.4. Calcium Imaging

2.8.5. Statistical Analysis

CHAPTER 3: RESULTS

3.1. Morpholino-mediated knockdown of Fmn2 leads to reduction in the RGC tectal innervation	30
3.2. Depletion of Fmn2 leads to decrease in the size of the neuropil and optic tectum.	38
3.3. Fmn2 morphants may show deficits in visually guided behaviours	41
3.4. Standardisation of Calcium imaging to visualise the activity in the optic tectum to a looming stimulus.	44

CHAPTER 4: DISCUSSION

4.1. Discussion	46
4.2. Future direction	50
Reference	51

List of Figures

Figure 1.1: Stages of Neuronal Development.

Figure 1.2: Growth cone cytoskeleton

Figure 1.3: Retinotectal pathway in zebrafish larvae

Figure 1.4: Retinotectal projection in the *Brn3c:mGFP* transgenic line.

Figure 3.1: Fmn2 morphants show reduction in arborization of axonal projection of RGC in the optic tectum.

Figure 3.2: Degree of variation in the reduced arborization phenotype in Fmn2 morphants at 3.5dpf.

Figure 3.3: Depletion of Fmn2 leads to reduction in the volume of the retinorecipient area SO and SFGS of optic tectum at different developmental time points.

Figure 3.4: The intensity by volume of the projection of the RGC to the optic tectum in Fmn2 morphants and control zebrafish larvae

Figure 3.5: Whole-mount immunostaining of Tg(Brn3c:GAP43-GFP) to visualize different regions in the optic tectum.

Figure 3.6: Decrease in the size of the neuropil and the optic tectum in the Fmn2 morphants at 4dpf.

Figure 3.7: Response of the zebrafish larvae to a moving dot stimulus.

Figure 3.8: Response index of the Fmn2 morphants and control zebrafish larvae.

Figure 3.9: Calcium activity of a 3dpf zebrafish larvae to a looming stimulus

Figure 3.10: Standardization of the calcium response of a 3dpf zebrafish larva to a looming visual stimulus.

ABSTRACT

Cytoskeletal remodelling is imperative for the formation of precise neural circuits. Formin2 (Fmn2) is a protein known to be involved in the remodelling of both actin and microtubule cytoskeletons. Fmn2 mRNA was previously shown to be enriched in the retinal ganglion cells (RGCs) as well as in the CNS of zebrafish larvae. The zebrafish retinotectal pathway is a model system for axon guidance and retinotopic mapping. In this study, we show that morpholino-mediated knockdown of Fmn2 in zebrafish leads to defects in the architecture of the axonal projections of the RGCs to the optic tectum. We find that Fmn2 is required for the development of the optic tectum as Fmn2 morphants show reduction in the optic tectum size. In order to evaluate the functional relevance of the structural defects observed, we have evaluated the behavioural response of zebrafish to moving stimuli. Preliminary results show a trend suggesting compromised response towards this visual cue in Fmn2 morphants. Further, we have developed and standardized calcium imaging protocols that will allow us to monitor the response of the optic tectum to visual cues. Our experiments suggest that Fmn2 is required for the development of the functional visual circuitry in zebrafish.

CHAPTER 1: INTRODUCTION

1.1 Neural Circuit development

The brain interprets sensory input from the external environment and elicits behavioural repertoire that is carried out by motor neurons. Neural circuits form the neural basis of the brain's multiple functional capacities. The neural circuits are made up of a cluster of neurons functioning together to elicit diverse functional roles spanning from the simplest reflex arc to complex cognitive processes (Tau and Peterson, 2009).

The brain is a highly organized organ that contains millions of axon tracts that are guided to their targets and form predictable connections. The development of a proper neural circuit is vital for the proper functioning of an organism. The development of neural circuits involves multiple stages, including axon–dendrite differentiation, axonal growth and guidance, synapse formation and maturation, and refinement of developing circuits (Weiner et al., 2013) (Figure 1.1). Neurons, the basic unit of a neural circuit, are highly polarised cells that have functionally and structurally distinct compartments: axons and dendrites. The neuronal polarization helps in the unidirectional flow of electrochemical stimulus through the circuit. The dendrite gathers the input signals, and the processed output signal is relayed to the target through the axon.

Any minor deviation from this complex and precise development of neural circuits could lead to neurodevelopmental disorders such as intellectual disability, autism spectrum disorders, and schizophrenia. The disintegration of the neural circuits is a known cause of neurodegenerative disorders like Alzheimer's or Parkinson's disease (Bossers et al., 2009; Gilman et al., 2012; Antonell et al., 2013; Iossifov et al., 2014; Pinto et al., 2014). The development of neural circuits is a complex process, and it is influenced by factors such as environmental events, genetic factors, as well as neuroplastic responses (Tau and Peterson, 2009). It is essential to know about the genetic, molecular, and cellular

mechanisms and players involved in the developmental process to understand neural correlates of such disorders.

1.2 Stages of neural circuit development.

The first process in the development of a neural circuit is the differentiation of axon and dendrites. In vitro studies in rat embryonic hippocampal neurons have shown the different morphological stages of neuronal polarization. The neurons, after the formation and differentiation, form filopodia like structures. The protrusions that have a growth cone at their distal tip further develop into the minor process or immature neurites. The immature neurites are morphologically similar and exhibit dynamic extension and retraction. The balance between extension and retraction of the neurite provides symmetry to the neuron in this stage. But this symmetry is lost as the neuron proceeds to the second stage where one of the neurites starts to extend rapidly giving rise to an axon and in the next stage, the other neurites mature to form the dendrites (Dotti et al., 1988, Arimura and Kaibuchi, 2007).

The growing axon has to navigate its way through the complex extracellular matrix to reach its appropriate target location and form synapse. The axon guidance is a complex and intricate process in which the growth cone plays a crucial role. This amoeboid-like structure was initially observed in 1890 by Santiago Ramón y Cajal in chick spinal commissural neurons. The growth cone, which is highly supported by actin, helps the axon reach the target location by responding to the intracellular and extracellular guidance factors (Cajal 1890; Tessier-Lavigne and Goodman, 1996; Chao et al., 2009; O'Donnell et al., 2009). These factors provide the spatial information for the growth cone to understand the complex and changing environment and guide the axons to the destined location. The steering of the axon based on the spatial information is regulated by the action of two cytoskeletal filaments that is present in the growth cone- namely actin and microtubule (Geraldo and Gordon-Weeks, 2009). The axon on reaching

stereotypical locations starts to branch so that they can innervate more than one target or sometimes different targets.

The axon on reaching the target location forms chemical synapses, which are the specialized junctions through which neurons signal to one another, with the target location. The formation of synapse involves a change in morphology as well as the structure of the cell (Shen and Cowan, 2010). These changes are dependent on the ligand-receptor interactions, intracellular signalling cascades, and complex filamentous actin (F-actin) remodelling. The initial overproduction of synapses is compensated by the removal of unused and weak synapses in an experience-dependent manner by a process called synaptic pruning (Adrienne L. Tierney and Charles A. Nelson, III, 2009).

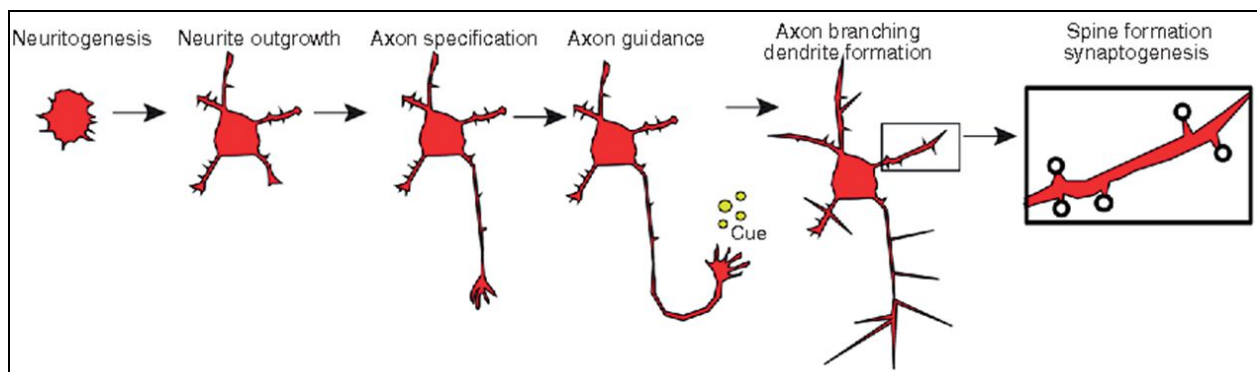


Figure 1.1: Stages of Neuronal Development.

Neurons go through stereotypical morphological stages throughout the development. The first stage is the neuritogenesis where small protrusions are formed in the membrane of the nascent neuron. This stage is followed by the elongation of protrusion in the neurite outgrowth stage. One of the protrusion polarizes to give rise to the axon. The specified axons are guided to the target location by extracellular cues. The formation of dendrite and axon-dendrite branching enables a single neuron to form multiple synaptic connections. Finally, synaptogenesis leads to the formation of nascent synaptic spines. (Adapted from (Winkle and Gupton, 2016))

The growth cone, which plays a pivotal role in the formation of neural circuits, is characterized by the presence of finger-like structures called filopodia and thin-sheets like lamellipodia (Dent et al., 2010). Both of these are actin-based structures with the former having unbranched actin filaments due to the absence of Arp2/3 and later having branched actin filaments (Dent et al., 2010). Growth cones also consist of a microtubule rich region that runs through the length of the axon (Lowery and Van Vactor, 2009). Cytoskeletal remodelling has a crucial role in the initial stage of neuronal development, which involves neuronal polarization and axon outgrowth.

1.2.1. Cytoskeletal Remodelling in the Neural circuitry

The different stages of neural circuit development depend on active and dynamic cytoskeletal remodelling (Menon and Gupton, 2016), which consists of neurofilaments, microtubules, and actin, regulated by cytoskeletal remodelling proteins such as the Formins, profilin. Each component of the axonal cytoskeleton has specific functions like the neurofilaments that help to maintain the axon radius and conductance, microtubules and actin are involved in the axonal specification, growth, and guidance (Kevenaar and Hoogenraad, 2015). The dynamic interaction between microtubule and actin regulates the continuous cytoskeletal remodelling. The distribution of actin filament and microtubule in the growth cone are mutually exclusive to some extent. Actin filaments are majorly found in the P-domain of the axon and microtubule in the axon shaft. But the region where cross-talk of the actin filament and microtubule happens is important for the turning of growth cones and axon growth. Actin forms filopodia and lamellipodia, dynamic regions of growth cones essential in driving guided cell motility (Dent et al., 2011). Actin regulators and signalling processes modulate the actin dynamics. During axonal polarisation and outgrowth, instability of the actin in the neurite enables the stable microtubule to protrude easily. Axon branching involves accumulation of actin filament. The accumulated actin filaments form the axonal filopodia. This is followed up by the invasion of the filopodia with MT and hence allows the axonal filopodia to mature

into collateral branches (Lasser et al., 2018). Several molecules like Rho GTPase and its downstream target Rho kinase, profilin are involved in the actin cytoskeletal remodelling (Dent et al., 2011).

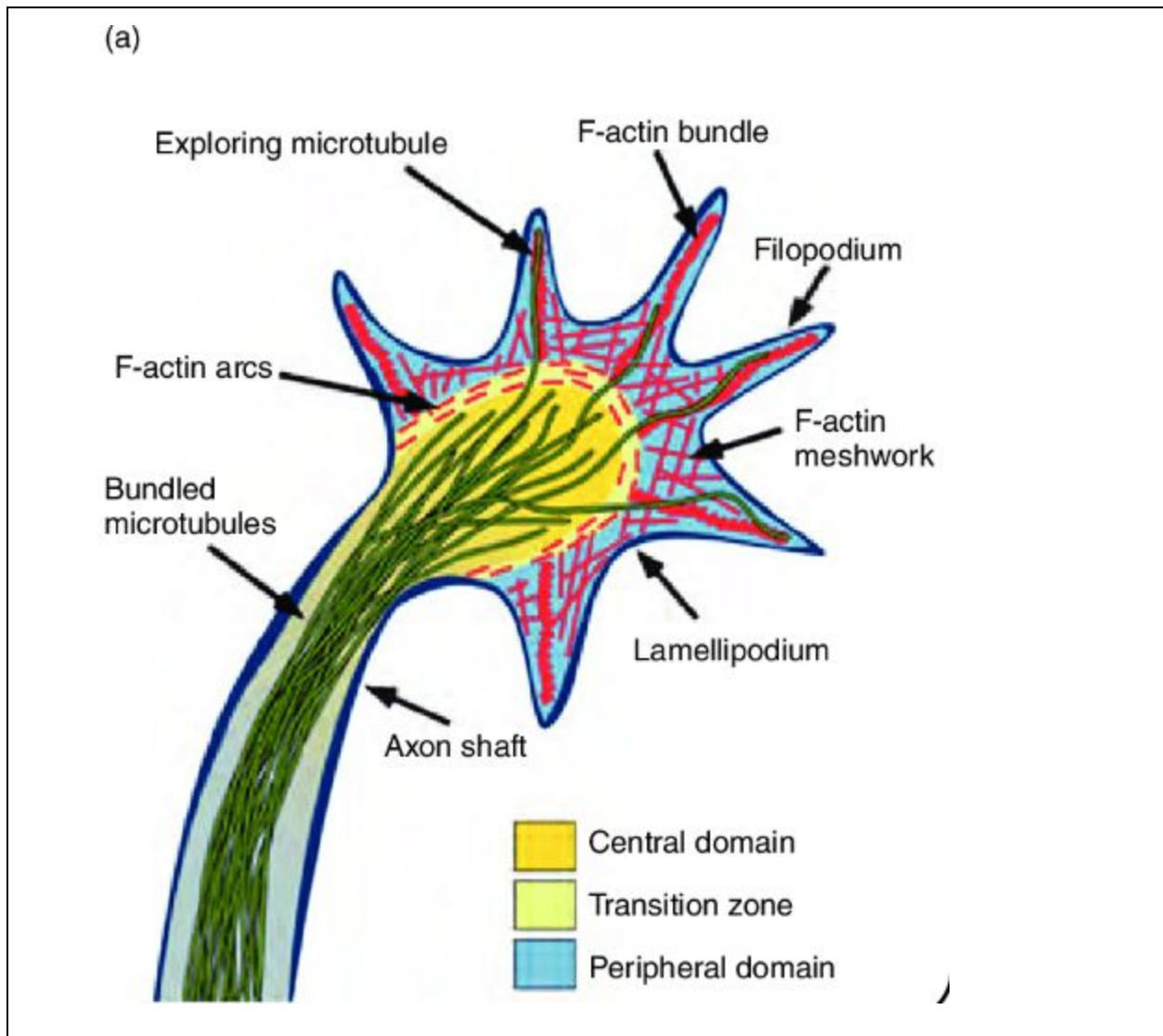


Figure 1.2: Growth cone cytoskeleton.

Growth cone is a dynamic structure present at the terminal of an axon. It has different morphological regions: peripheral domain (P-domain), transition domain (T-domain) and central domain (C-domain). The P-domain consists of the dynamic region of the growth cone with filopodia and lamellipodia. The filopodia are rich in F-actin bundles

and lamellipodia with F-actin meshwork. The microtubules(green) at the axon shaft are bundled parallelly. At the C-domain, the microtubules are not held together and they start to extend separately towards the P-domain. The individual microtubules align alongside F-actin bundle(red). Adapted from (Letourneau, 2016)

1.2.2. Formin-2

One family of protein which is involved in the cytoskeletal remodelling by regulating actin and microtubule dynamics are the Formins. Most members of the Formin family have an FH1 and FH2 functional domain. Fmn2 is a member of the Formin family. In addition to the FH1 and FH2 domain, the C- terminal of Fmn2 has an FSI(Formin Spire Interaction) domain at the tail. The highly conserved dimeric FH2 domain is associated with the actin polymerization dynamics and also in de-novo actin polymerization. (Higgs 2005). Recent discoveries have indicated the role of the FSI domain of Fmn2 in actin bundling and microtubule interaction. Studies in spinal neurons have shown that Fmn2 is involved in the stabilization of microtubules in growth cones (Kundu et al., 2020).

Fmn2 mRNA is predominantly enriched in the CNS of mammals, chick as well as zebrafish(Leader and Leder, 2000; Schumacher et al., 2004; Unpublished data, Dhriti Nagar). *In vitro* studies in fixed chick spinal neurons have shown the importance of Fmn2 in retaining neuronal morphology. Also, it has shown knockdown of Fmn2 affected filopodial number, growth cone motility, and growth cone area(Sahasrabudhe et al., 2016). These phenotypes were rescued using mouse ortholog of Fmn2 in the chick neurons, hence implying that Fmn2 is essential in the growth cone maintenance. They have shown that Fmn2 as a necessity for commissural neuron outgrowth and pathfinding(Sahasrabudhe et al., 2016). Fmn2 maintains the actin bundles, which is necessary for the stability of adhesion in growth cone filopodia. Axonal branching studies in chick spinal neurons have shown that Fmn2 mediated actin nucleation and elongation essential for the formation of protrusions in axon shafts (Das and Kundu).

Studies have shown that Fmn2 is downregulated in aged mice, and de novo mutations in Fmn2 can lead to intellectual and cognitive disabilities in humans (Law et al., 2014; Gräff, 2017). Experiments on young mice have shown that lack of the Fmn2 gene exhibits PTSD-like phenotypes and corresponding impairments of synaptic plasticity, whereas new memories are appropriately consolidated. Agís-Balboa and his colleagues have observed the Fmn2 expression level in post mortem brain samples of Alzheimer's patients. They have shown the deregulation of Fmn2 in PTSD and Alzheimer's disease (AD) patients (Agís-Balboa et al., 2017). In order to understand the neural correlates of these disorders, it is necessary to understand how Fmn2 affects the neural circuit development *in vivo* in a vertebrate model.

1.3. Zebrafish as a model organism

Zebrafish is a shoaling tropical fresh-water fish that belongs to the Teleostei infraclass, a monophyletic group (Amores et al., 2011). Usage of zebrafish as a model organism dated back to the late 1950s. They have become a powerful model organism in different fields like vertebrate genetics, development, regeneration, and toxicology.

The usage of both adult and zebrafish larvae for neuroscience has increased as it enables us to understand how the higher centre of the brain works in diseased conditions. This growth in usage is because zebrafish is a vertebrate species with high physiological and genetic homology to humans. Further, the ease of genetic manipulation and a similar central nervous system (CNS) morphology to humans makes them perfect for studies on the brain (Kalueff et al., 2014). Several reasons contributed to the popularity of this model organism, like the ease of care, fecundity, rapid development, small size, and ease of manipulation. The Zebrafish life cycle has distinct stages, which makes it easy to look at different circuits throughout its development. Zebrafish are amazing breeders, giving up to a few hundreds of eggs each week. Their development is very rapid, and they start to elicit complex behaviours as early as 4 days post-fertilization(dpf).

The transparency of the eggs enables manipulation of the functioning of any convenient protein by injection of morpholinos, peptic nucleic, or short siRNAs at the single-celled stage of the embryo and monitoring development of the larvae. The development of efficient transgenesis techniques leads to the generation of a vast number of transgenic fish lines, in which fluorophores are expressed in a spatial as well as temporal pattern in the CNS (Baier and Scott, 2009). Also, genetically encoded calcium indicator (GECI), GCamp transgenic zebrafish line along with improved optical techniques enabled successful visualization of neuronal activity, at single-cell resolution (Nakai et al., 2001; Akira Muto and Koichi Kawakami, 2013). The dimension of a brain of a zebrafish larvae at five days post fertilization (dpf) is less than 500 μm in thickness and 1.5 mm long, making virtually all neurons accessible to multiphoton microscopy *in vivo* (Rainer W.Friedrich Gilad A.Jacobson PeixinZhu, 2010). Zebrafish has a rich behavioural repertoire, which provides insights into neural pathways and circuits (Kalueff et al., 2013).

1.4 The retinotectal projection

The retinal ganglion cells (RGCs) are the primary cell type in the innermost cellular layer of the retina. They are the primary output source of the visual information from the eye to the brain. There is a connectivity map between the retina and the different target regions in the zebrafish. (Robles et al., 2014). They have shown that there are at least 50 morphologically distinct types of RGCs based on the morphology of their dendrites and axonal projection pattern in the midbrain. The RGC in the same dendritic morphology type can have a different axonal projection. Robles et al. showed that the RGCs project their axons collaterals to more than one visual area (Robles et al.,2014). The RGCs project their axons in a retinotopic manner. The axons of the RGC which are located at the nasal region of the retina project to the caudal side of the tectum and the temporal axons arborize in the rostral part of the tectum. Likewise, dorsal axons target the lateral tectum and ventral axons travel to the medial tectum (Kita et al., 2015)(Figure

1.2). The retinotectal projection in zebrafish is used as a model system for deciphering the mechanism underlying axonal guidance as well as pathfinding (Xiao T, 2005).

The first RGCs are born at 28 hours post-fertilization(hpf), and they start to extend axons, which initially grow within the retina. They exit the retina at the Optic Disc(30–32hpf) (Hu and Easter,1999). The fasciculation of the RGC axons forms the optic nerve. They are guided toward the ventral midline of the diencephalon. The nerves coming from both eyes meet to form the optic chiasm(34–36hpf) (Stuermer,1988). Unlike other higher vertebrates, zebrafish lack binocular vision, so all the axons that cross the ventral midline are projected towards the contralateral optic tectum, their main synaptic target in the midbrain. By 48hpf, the axons of the RGCs are projected to the contralateral tectum to form the retinotectal pathway in a retinotopic and precise manner (Stuermer,1988). After crossing the midline, the axonal fascicules starts to selectively defasciculate at different throughout till they reach the optic tectum. The initial guidance of the RGCs axons to different arborization fields happens in an activity-independent manner (Stuermer,1988). Guidance cues such as netrin, Slits, and ephrins play a vital role in guidance (Erskine and Herrera, 2007).

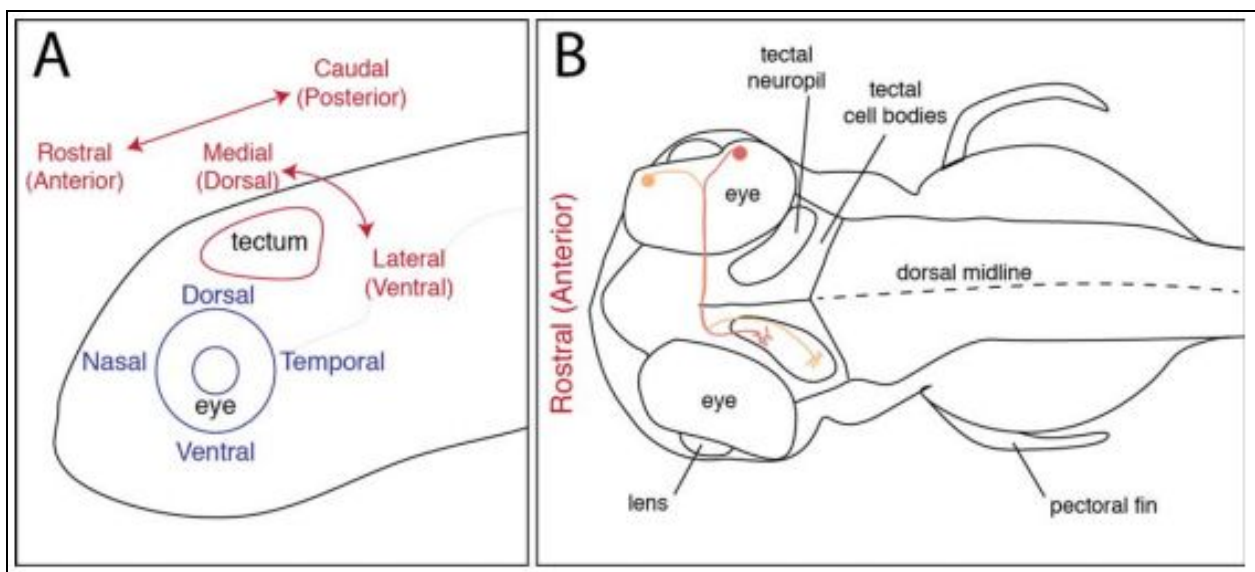


Figure 1.3: Retinotectal pathway in zebrafish larvae. (A) Schematic representing the lateral view of the zebrafish larvae with anatomical terms.(B) The dorsal view of the larvae shows the topographic map. The axons of the RGC which are located at the nasal side (orange) of the retina project to the caudal side of the neuropil and the temporal axons (red) project to the rostral part of the tectum. Likewise, dorsal axons target the lateral tectum and ventral axons travel to the medial tectum. (Adapted from Kita et al., 2015)

1.4.1 Central projections of RGCs

Burrill and Easter have identified nine retinorecipient nuclei in the zebrafish midbrain other than the optic tectum by intraocular injection of lipophilic fluorescent dye. The dye injection enabled to trace the RGC axons. These retinorecipient nuclei, along with optic tectum, are known as the arborization fields referred to as AF1 to AF10(Figure 1.3 (B)). Specific RGCs types like the direction and orientation-selective project their axon to either one or multiple AFs and make synapses in the target cells that have projected their dendrites to the AFs hence establishing a map of the visual field in the brain (Burrill and Easter, 1994). One or few of the AFs act together to perform a particular visual behaviour, but the role of all the AFs in different behaviour is not known completely (Kubo et al., 2014; Semmelhack et al., 2014). Ablation experiments of AF 7 have shown that impairment in prey capture behaviour and calcium imaging has shown the activity in AF7 against the prey-like visual stimulus, which shows that AF7 is a crucial component of the prey detection circuit (Semmelhack et al., 2014; Robles et al.,2014). AF1 probably has a role to play in Visual background adaptation and Circadian photoentrainment. Other studies have shown that direction-selective neurons in which envelope AF7 are involved in OKR-like behaviour and global optic processing (Roeser and Baier, 2003; Kubo et al., 2014). A vast majority of the axonal projection of the RGC terminates in the optic tectum (Robles et al., 2014)

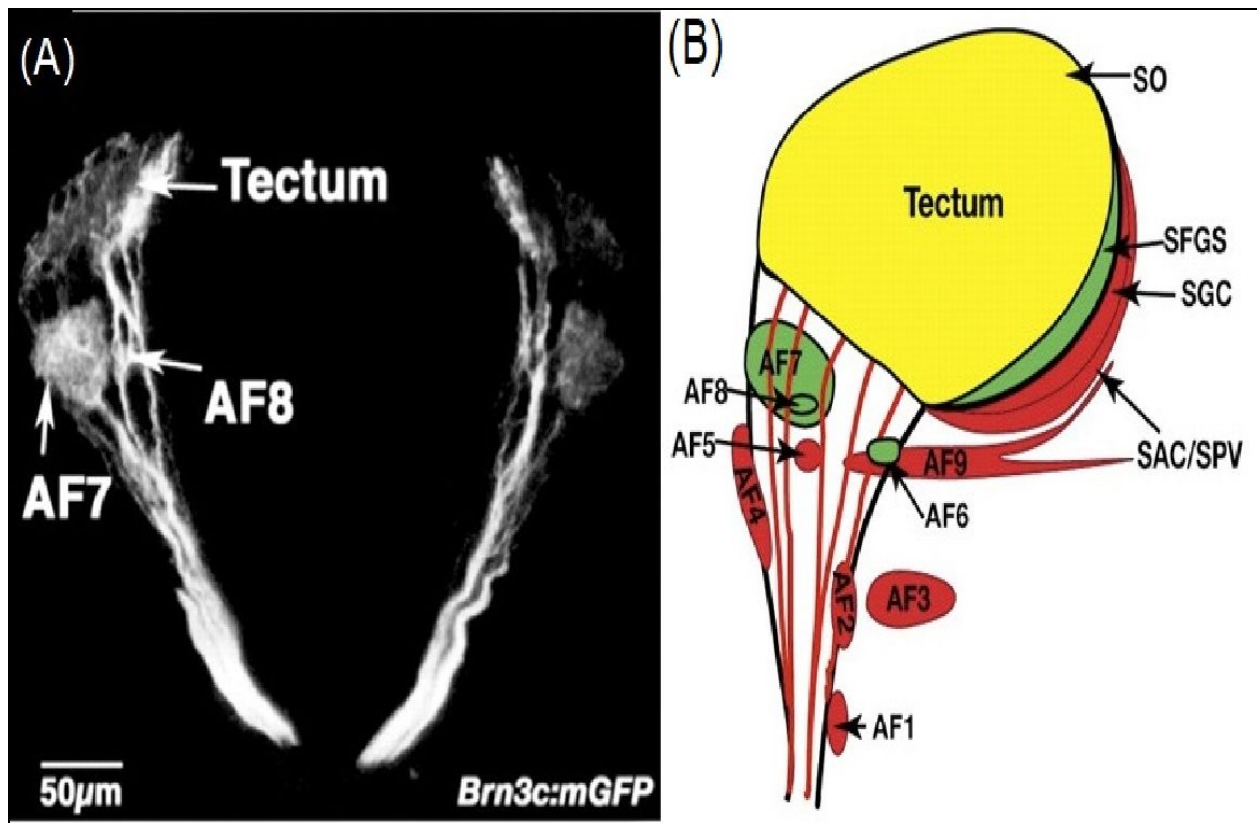


Figure 1.4 Retinotectal projection in the *Brn3c:mGFP* transgenic line.

(A) Transverse section of *Brn3c:mGFP* transgenic line. (B) Schematic representation of the retinotectal projection including the ten arborisation fields. AF10 is the largest and it has 4 main layers. In *Brn3c:mGFP*, GFP is expressed in SFGS and SO layers of the optic tectum, AF7, AF8 and AF9. Red regions are devoid of GFP expression, the yellow region has weakly innervated *brn3c* positive RGCs and green represents a strong expression of significant inputs from *Brn3c:mGFP*. Adapted from (Xiao, 2005)

1.4.2. Optic Tectum (AF 10)

Zebrafish tectum is located at the roof of the midbrain and is accessible to optical imaging, observing neuronal activity, ablations, and electrophysiology. The zebrafish tectum consists of two regions: the neuropil, which consists of the retinal afferents, dendrites, and axon projected from the tectal neurons as well as some tectal

interneurons and the deep cell body layer, the stratum periventriculare (SPV) (Linda M Nevin, 2010). The zebrafish optic tectum is similar to the Superior colliculus of humans. It is the most significant retina recipient area in zebrafish midbrain, with around 97% of the RGC projecting their axons and innervating different layers (Robles et al., 2013; *Burrill JD, Easter SS Jr, 1994*). The formation of lamination in zebrafish is similar to that of retinotectal axons seen in many vertebrates, varying from birds to mammals (Huberman et al., 2010). The axonal projections of RGCs innervate 10 clear laminates. These layers are arranged like one above the another: the superficial layer, the stratum opticum(SO) and its two sub laminae, the stratum fibrosum et griseum superficiale (SFGS), which in turn splits into six sub laminae, the stratum griseum centrale (SGC) and finally the deepest layer stratum album centrale (SAC) and the stratum periventricular (SPV) (Meek J, 1983; Roeser, T. & Baier, H., 2003; Robles et al., 2013)(Figure 1.3 (B)). The RGCs from the ventral retina terminate in the dorsal side of the contralateral tectum and vice versa, and the anterior tectum is innervated by axon from the temporal retina and vice versa. Thus the axons are projected in a retinotopic manner (Robles et al., 2014). Other than the sensory afferent, tectum also receives inputs from different sensory systems like the auditory, lateral line, somatosensory. These inputs help in the formation of sensory maps in the deeper layers of the tectum (Nevin et al. 2010).

Using the Golgi studies and UAS/ Gal4 transgenic approach, about 15 morphologically distinct tectal cells are identified based on different criteria like soma location, dendritic and axonal arbors (Meek and Schellart, 1978; Scott and Baier, 2009). The tectal neurons include the periventricular interneuron and projection neurons (PVN) in the stratum periventricular, superficial interneurons in the neuropil, intertectal neurons (Scott and Baier, 2009; Robles et al., 2011; Gebhardt C et al., 2019). Distinct tectal neurons are tuned to different behaviorally relevant visual stimulus parameters. A population of periventricular interneurons is responsible for the orientation of the larvae towards small objects (Barker.A and Baier H, 2015). The periventricular neurons have

their efferent axons in premotor and motor areas (Nevin et al. 2010). SInNs size filters the incoming visual circuit in prey capture behaviour (Del Bene et al. (2010)) whereas the intertectal neurons are involved in the binocular localization of prey (Gebhardt et al., 2019). The visual information from the eyes is transmitted to the deep layers of the optic tectum, from where it is delivered to different motor centres of the mid and hindbrain to elicit the appropriate behaviour.

1.5.Zebrafish visual behaviours

The zebrafish larvae are free-swimming organisms and are prone to predation, so their visual system develops very rapidly, and the larvae start to elicit simple visual behaviour like the response to light as early as 3dpf. The visual system becomes fully functional by 5dpf, and they are highly dependent on the vision to perform multiple complex behaviours (Gonzalo G. De Polavieja. and German Sumbre., 2014). Most visual behaviours can be generated by using virtual visual stimuli during laboratory experiments (Bianco IH 2011, Trivedi and Bollmann, 2013). Visual mediated behaviour in zebrafish larvae includes prey-capture, the optomotor response (OMR), the optokinetic response (OKR), escape response (Orger and de Polavieja, 2017). Ablation studies have shown that OKR and OMR response in zebrafish larvae doesn't depend on the functioning of the tectum (Roeser and Baier, 2003). Optic tectum is essential in the prey capture response and escape response (Gahtan et al., 2005; Temizer I, 2015).

Zebrafish are also hunted in nature by different types of predators like adult fish and birds. So they exhibit an escape response against the approaching predator. A robust avoidance response is evoked by the freely swimming zebrafish larvae on the display of a large dot moving back and forth below the chamber (Colwill and Creton, 2011). As an object approaches, the angle it subtends on the retina grows from a small dot to a larger one. The response of zebrafish larvae can be replicated by a looming stimulus, which can be artificially given by an expanding dark spot in a white background. This looming stimulus mimics an approaching predator or an imminent collision. Looming- triggered a

response in zebrafish larvae mainly consists of two distinct phases, first is the high amplitude contralateral bend of the tail, followed by the fast burst swim (Temizer I, 2015). Three regions of the AFs: optic tectum, AF6, and AF8 respond when a looming stimulus is provided. Ablation of the RGC axons in the tectal neuropil leads to a reduction in the escape response, which shows that proper tectal functioning is necessary for the circuit (Temizer I, 2015).

1.6. Motivation

Studies in the lab showed the enrichment of Fmn2 mRNA in the RGCs of the zebrafish larvae along with the CNS. Studies in chick spinal neurons have shown the importance of Fmn2 in axonal outgrowth and pathfinding, as well as axonal branching. This prompted me to investigate the role of Fmn2 for RGC outgrowth, targeting, and function.

CHAPTER2: MATERIALS AND METHODS

2.1. Zebrafish Handling

Embryos were raised in Danieau's solution (17 mM NaCl, 2 mM KCl, 0.12 mM MgSO₄, 1.8 mM Ca(NO₃)₂, 1.5 mM HEPES) at 27.5°C on a 14/10 light/dark cycle. Transgenic lines Tg(Brn3c: GAP43-GFP) larvae were used for behavioural experiments and confocal imaging, and Tg(Elavl3: GCamp6f) larvae were used for Calcium Imaging. Larvae used for imaging were treated with 0.003% 1-phenyl-2-thiocarbamide (PTU) from 1 dpf to reduce pigmentation of the retina.

2.1.1. Transgenic lines

2.1.1.1. Tg(Brn3c: GAP43-GFP)

Tg(Brn3c: GAP43-GFP) expresses membrane-targeted GFP under the *brn3c* enhancer element. The subset of RGCs that express Brn3c:GAP43-GFP have their axons innervating SFGS and SO layers of the optic tectum, and sparsely innervates AF-6, AF-7 and AF-8. Other than the RGCs, the transgene also labels the neuromast of the lateral line(Xiao, 2005)(Figure 1.3 (A)).

2.1.1.2. Tg(Elavl3: GCamp6f)

Tg(Elavl3: GCamp6f) expresses the genetically encoded calcium indicator (GECI) which was created from a fusion of green fluorescent protein (GFP), calmodulin and M13, GCamp6f under the cytosolic *elavl3* promoter, which provides near-pan neuronal expression.

2.2. Embryo microinjection -Morpholino Injection

Kwik-fil standard borosilicate glass capillaries were pulled on a micropipette puller. The pulled capillaries were broken to a narrow tip with sharp forceps under a stereomicroscope. In the Pico-Injector Microinjection System from Harvard Apparatus capillaries the injection is produced by air pressure with compressed nitrogen. The

injection pressure, together with injection time determine the volume of the morpholino that is injected into the cell. The injection pressure varied between 15-20 PSI. The injection pressure was calibrated by checking the injection volume. Discharging the morpholino to a 35mm petri plate containing mineral oil enabled us to measure the injection volume under a stereomicroscope with a scale in one of the eye-piece. The fertilized zebrafish eggs were placed in the trenches of an agarose microinjection chamber. 2nL of Splice-blocking morpholino and control morpholino was injected in the single-celled stage of zebrafish larvae for each experiment. Splice-blocking morpholino leads to the insertion of an intron between exon5 and exon6, and the inserted intron has a stop codon in the sequence, this leads to the formation of non-functional Fmn2 protein in the larvae.

Control morpholino 5'-CCTCTTACCTCAGTTACAATTTATA -3',

Fmn2 Splice Blocking morpholino 5'-ACAGAAGCGGTCATTACTTTTTGGT -3'

2.3. Live Imaging

Confocal images of the axonal projection of the RGC to the optic tectum were taken at different developmental timepoints to look at the architecture of the projection. PTU treated larvae were screened for GFP at 2dpf. Before imaging, they were embedded in a coverslip bottom Petri plate in 0.8% low melting point agarose(LMPA) dissolved in E3 medium containing 0.3% tricaine. The larvae were mounted with the dorsal side of the larva near to the coverslip bottom.

2.4. Whole-mount immunostaining.

Zebrafish larvae at 3,4 and 5 dpf were used for the whole-mount immunostaining against GFP. The larvae were initially anaesthetised and fixed with 4% PFA, 4% sucrose for 4 hours at room temperature(RT), then transferred to phosphate-buffered saline(PBS) and kept at 4°C, overnight. The larvae were dehydrated through 50% methanol in 0.5% PBST to 100% methanol. It was kept at -4°C for a minimum of 16 hours. The larvae were washed using 50% methanol in 0.5% PBST to rehydrate the

tissue. The rehydration was followed by wash steps using PBST (4 x 5min). Further for the epitope retrieval, they were digested with Proteinase K (40ug/ml) for 20mins, then re-fixation was performed using 4%PFA for 20min. After fixation, the PFA was removed thoroughly by washing with PBST (4 x 5min).

Before incubating the samples with primary antibody (Chicken anti-GFP, 1:500, Abcam), the samples were transferred to blocking solution (10% HIGS, 1% DMSO in PBST) at RT. After 1 hour of blocking, the samples were kept in primary antibody diluted in the blocking solution at 4°C overnight. The next day, the samples were rinsed with PBST multiple times before PBST washes (4 x 5mins). Then samples were incubated using anti-chicken Alexa- Fluor 488 diluted in the blocking solution and kept at 4°C overnight. The following day, samples were initially washed (4 x 5min) using PBST after rinsing them with PBST, then incubated with PBST containing DAPI. The samples were transferred to a mounting medium containing glycerol and DAPI. The samples were then mounted in 0.8% agarose with the dorsal side closer to the coverslip of a coverslip bottom Petri plate.

2.5. Imaging

For both live and fixed zebrafish larvae, confocal imaging was performed using a Zeiss LSM 780 microscope with associated ZEN software. z-stacks were captured using 25x/0.8 oil immersion objectives with appropriate lasers and z-stack parameters.

2.6. Behaviour Assay

A single larva was placed in a 24-well plate (diameter= 16.2mm). The chamber was placed on the screen of a laptop. A python-written code was used to generate the visual stimuli. A CCD camera (Pike F-032B, Allied Vision Technologies(AVT), Germany) was positioned above the 24-well plate and focussed on the well containing the zebrafish larvae using a clamp stand, to record the movement of the larvae during the behavioural experiment.

Moving dots(12-pixel radius) were presented from a random direction but there will be only one dot at the screen at one time. The dots were presented for 1 minute to ensure minimum 6 larva-dot interactions. The dots were moving at a rate of 30 pixels per second. Behaviour experiment was performed on 5dpf control and morphant zebrafish larvae. All other light sources in the behaviour room were switched off during the experiment to make sure that the computer screen was the only source of light. All experiments were conducted during the day time and the water level in the well was kept the same for all samples throughout the experiment. Images were acquired using AVT_Smartview software (Allied Vision Technologies) at 60fps.

2.7. Calcium Imaging

For recording the calcium activity in the optic tectum, 3dpf *Tg(elavl3:GCaMP6f)* larvae were embedded in 2.5% low melting point agarose. The time-series recording of the calcium imaging was performed on Leica -- multiphoton microscope with 25x/1.05 objective. The wavelength of the excitation light was tuned to 920nm. Image acquisition was acquired using LAS X software. Time series were recorded with a spatial resolution of 520x300 pixels at 6.45 fps. Before initiation of the experiment, different morphological landmarks are identified and the z-plane for recording is decided based on the landmarks. Before recording the response to the looming stimulus, spontaneous activity of the z-plane is recorded for 160s (without any stimulus). A minimum of recording from two different depths was taken with intervals of 10-15mins.

The stimulus was displayed on an OLED screen (128x64) using an Arduino set-up connected to the laptop. The looming stimulus was displayed at a distance of approximate 0.5cm from the zebrafish larval eye. The stimulus started with radius, $r=0\text{cm}$ to $r=0.625\text{cm}$ over a time of 10s. After one trial of the stimulus was given, there was a 20 interval between trials for 160s.

2.8. Analysis

2.8.1. Live imaging: For live imaging of *Tg(Brn3c:GAP43-GFP)*, z-stacks were processed using Imaris (version) software. The 'surfaces' parameter provided by software gives a computer-generated representation of a specified grey value range in the data set. The software reconstructs the 3-dimensional image from the confocal stacks. The boundaries of the 3-D reconstruction are manipulated to crop the regions other than the RGC tectal innervation.

By controlling the threshold voxel intensity in the "surface" parameter, the software selects the voxels containing intensity above the set threshold and provides a computer-generated representation of the region. The software generates the volume, total voxel intensity, area, ellipticity along with many other parameters of this representation.

2.8.2. Whole-mount immunostaining: For the whole-mount immunostaining experiments, the confocal stacks were processed into maximum intensity projection(MIP) using ImageJ for quantification. Tectal innervation, neuropil and total volume of the optic tectum were determined by the MIP of the anti-GFP antibody stained tecta and the DAPI stained larval brain. The boundaries were traced to determine the area of the labelled regions.

2.8.3. Behaviour Assay: To analyse the behaviour experiments, the larval-dot interaction was observed. The initial nine dot-larva interactions were collected. A response was scored when the larvae generate a rapid movement when the moving dot is within the central 200° of its visual field. A no response was noted when the dot is within its central visual field but the larva doesn't respond. The interaction was quantified in terms of the response index (R.I.) = (the number of avoidances) divided by (the total number of larva-dot interactions)(Barker and Baier, 2015).

2.8.4. Calcium Imaging: For calcium imaging, the peak $\Delta F/F$ values were extracted using ImageJ. ROIs for single cells that showed activity during the visual stimulus were marked. The fluorescence intensity of the selected ROIs in the background(F_0) and response to the stimulus was measured from the time series recorded before and after the display of visual stimulus respectively. The relative fluorescence intensity and peak $\Delta F/F$ of each frame were calculated from the above values.

2.8.5. Statistical Analysis: All statistical comparisons for the plots were made using the Mann-Whitney non-parametric t-test in Prism 8 software.

CHAPTER 3: RESULTS

3.1. Morpholino-mediated knockdown of Fmn2 leads to a reduction in the RGC tectal innervation.

Previous studies have shown that Fmn2 is a necessity in axon outgrowth and guidance (Sahasrabudhe et al., 2016). It was also shown the Fmn2 plays a role in the axonal branching (Unpublished data, Sooraj Das). As there is a prominent expression of Fmn2 mRNA in the zebrafish RGCs, I investigated how depletion of Fmn2 affects the development of the zebrafish retinotectal pathway.

To determine defects in RGC axon outgrowth or branching due to depletion of Fmn2 expression in the larvae, we used the transgenic line *Tg(Brn3c:GAP43-GFP)* which strongly labels the SFGS and weakly labels SO layers of the optic tectum, and sparsely labels AF-6, AF-7 and AF-8 and the neuromast of the lateral line (Xiao, 2005).

The Fmn2 expression was depleted by morpholino mediated knockdown. Splice-blocking morpholino(MoSb) was injected in *Tg(Brn3c:GAP43-GFP)* at the single-celled stage to knockdown the Fmn2. As a control, a standard morpholino (MoC) was used. The splice blocking morpholino modifies the normal pre-mRNA splicing process by blocking the splicing sites. This leads to insertion of an intron between exon 5 and exon6 to the modified mRNA which contains a stop codon in the sequence. This led to the formation of a truncated protein. The standard control morpholino doesn't produce any change in the protein. The efficiency of the splicing can be assayed by RT-PCR as the insertion of an intron will show a change in the size of band in the RT-PCR product band on an agarose gel. We have observed that the morpholino mediated knockdown persists during the development of RGCs and results in permanent deficits in the circuitry.

The control and Fmn2 morphant Brn3c zebrafish larvae were mounted on a coverslip-bottom Petri plate with the dorsal side towards the coverslip at 3dpf, 3.5dpf, 4dpf, 5dpf and 7dpf. The z-stacks of the mounted zebrafish larvae were imaged using a confocal microscope. A 3D rendering of the z-stacks was obtained using imaris software and the intensity and volume of the brn3c positive RGC axons that innervate the optic tectum were quantified. There was an observable (**Figure 3.1**) and quantifiable(**Figure 3.3**) reduction in the arborization of the axonal projections of the RGC to the optic tectum at different developmental timepoints.

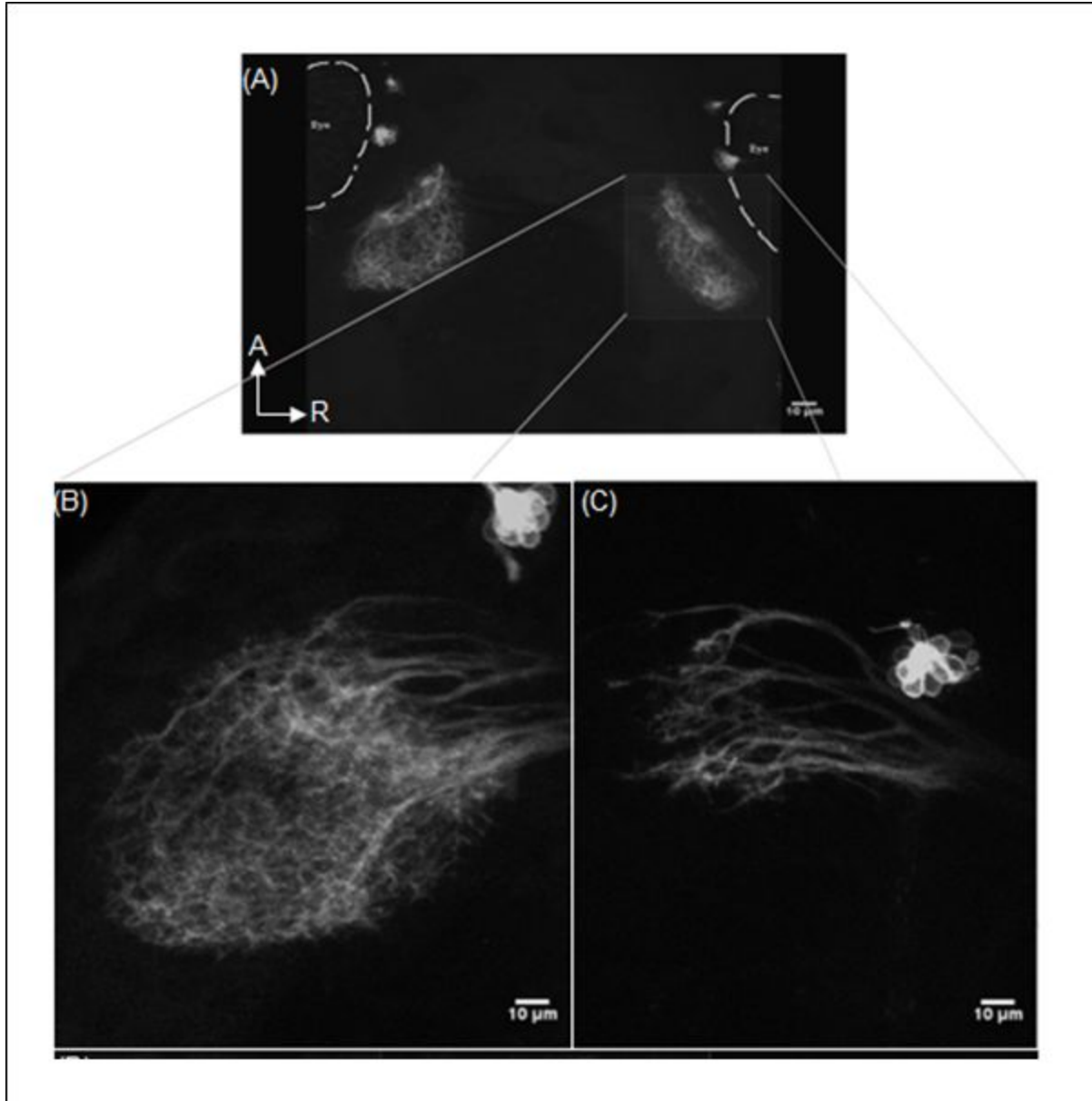


Figure 3.1: Fmn2 morphant larvae show a reduction in arborization of axonal projection of RGC in the optic tectum. (A) Expression pattern of Tg(Brn3c:GAP43-GFP) in a 3.5dpf uninjected zebrafish larva. The dotted lines represent the position of the eye. The enlarged image shown is the optic tectum of **(B)** control and **(C)** splice-blocking morpholino injected 3.5dpf zebrafish larva.

But not all the Fmn2 morphant showed the same degree of reduction in the arborisation of the RGC tectal innervation. The **(Figure 3.2 (A))** shows three different degrees of arborization at the 3.5dpf MoSb zebrafish larvae, in some cases, we see a delay in arborization as most of the axons have only reached their target while in some they are similar to the control. **Figure 3.2(B)** shows the penetrance of the phenotype in the MoSb zebrafish larvae. The below 25 percentile are those Fmn2 morphants which showed a delay in the RGC axons reaching the optic tectum and have just started to arborise. The between 25 and 75 is the group that has the volume of the brn3c positive RGC tectal arborise around the mean value. The above 75 percentile group has the volume innervated by the RGC axons within the range of the mean of the MoC zebrafish larvae.

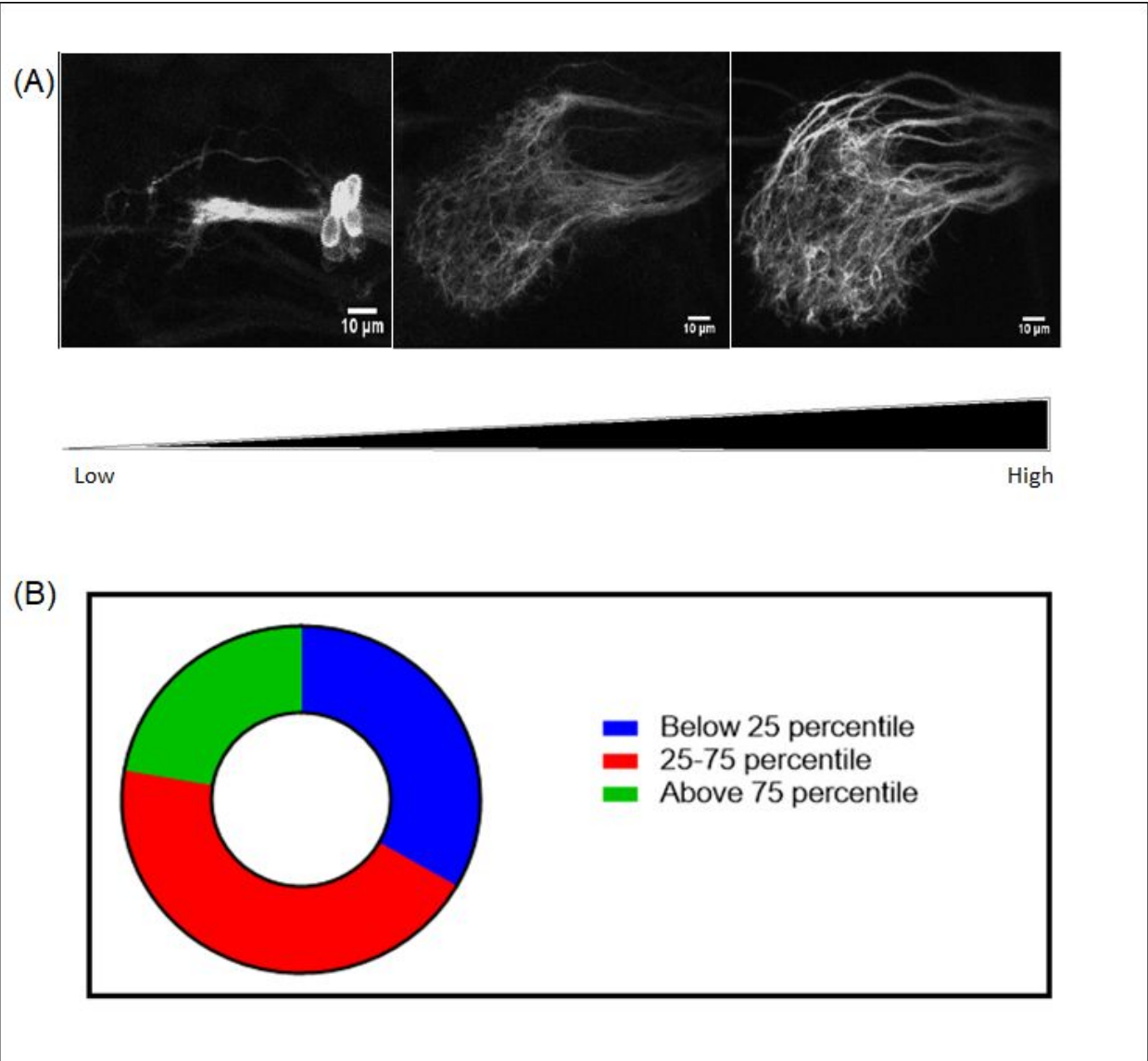


Figure 3.2: Degree of variation in the reduced arborization phenotype in Fmn2 morphants at 3.5dpf.

(A) The different degree to which the reduced arborization phenotype is observed in the zebrafish larvae at 3.5dpf. **(B)** Donut graph to represent the distribution in different ranges of arborization in the MoSb at 3.5dpf. The below 25 percentile represents the MoSb in which the axons just reach the tectum and start arborization (**Figure 3.2 (A) low**), above 75 percentile represent the MoSb that have arborization similar to that of the control (**Figure 3.2 (A) high**) and Between 25 and 75 percentile represent the

MoSb having intermediate arborisation.(Below 25 percentile: 6; Between 25-75 percentile: 8; Above 75 percentile: 4).

The innervation of the axonal projection of the *brn3c* positive RGCs to the tectum of the zebrafish larvae was quantified in terms of the volume of the RGC tectal innervation obtained from the 3D reconstruction of the z-stacks. From 3dpf to 5dpf, when the RGC axons in the control larva have reached and innervated the optic tectum, *Fmn2* morphants show a significant reduction in RGC axon tectal innervation at all developmental stages observed (**Figure 3.3**). The reduction in the volume arborised by the RGC tectal axons in the MoSb as compared to the MoC was at the maximum at 3.5dpf. This reduced volume of arborization phenotype is still observed in the late developmental stage i.e. 7dpf when the retinotectal pathway is formed and the larva can elicit visual guided behaviour.

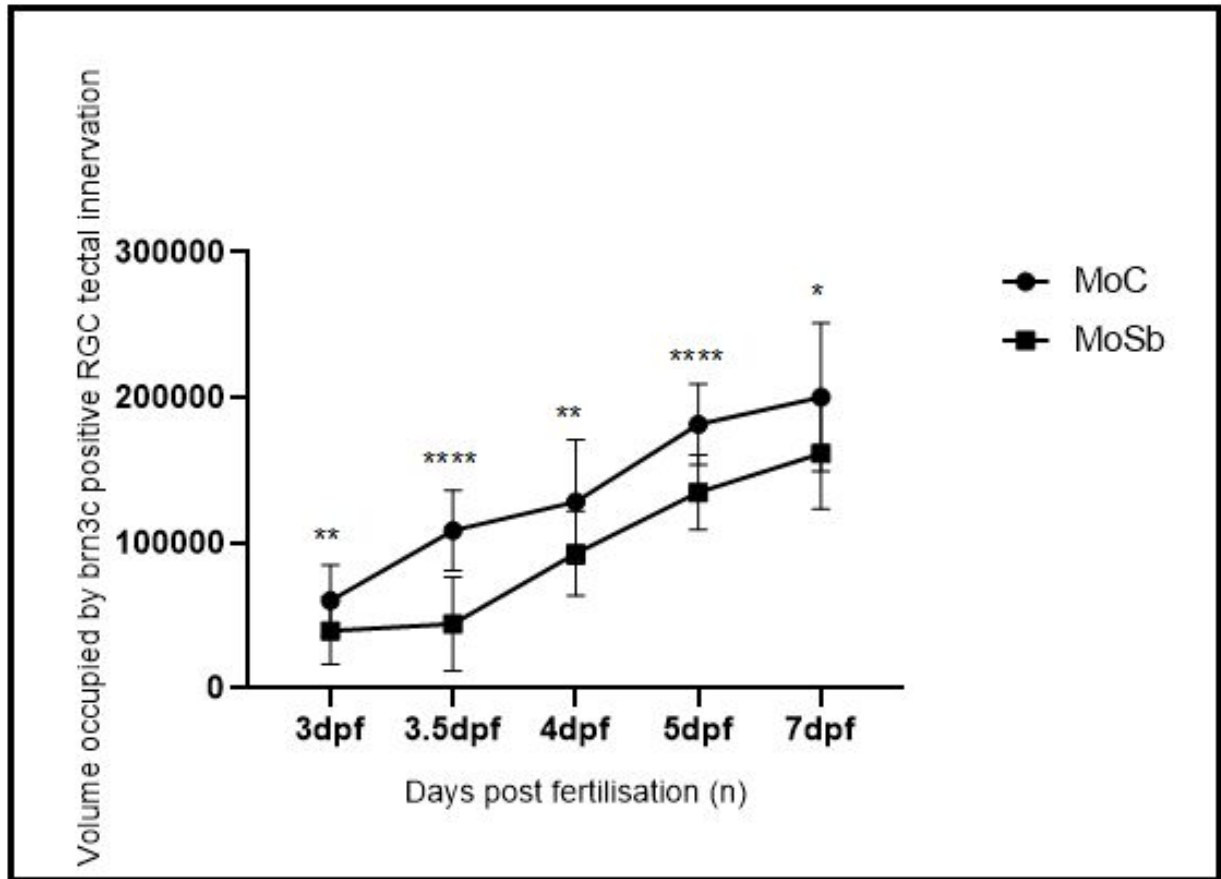


Figure 3.3: Depletion of Fmn2 leads to a reduction in the volume of the retinorecipient area SO and SFGS of optic tectum at different developmental time points.

Graph representing the tectal innervation as a function of volume from the 3D reconstruction of confocal images of live control and morpholino injected zebrafish larvae. The filled circle and square represents control morpholino and splice blocking morpholino injected zebrafish larvae at 3dpf (n= 25,MoC ; 25,MoSb ; p=0.0059), 3.5dpf (n= 25,MoC ; 18,MoSb ; p<0.0001%), 4dpf (n= 18,MoC ; 20,MoSb ; p=0.0043), 5dpf (n= 20,MoC ; 24,MoSb ; p<0.0001%) and 7dpf(n=18,MoC ; 21,MoSb ; p=0.0148). Mann-Whitney non-parametric test.

The reduced volume of the tectal innervation may be due to the reduced axon outgrowth or due to reduction in the extent of innervation. Tectal innervation measured as a function of the voxel intensity was normalised to the volume of the tectal innervation to get a measure of the extent of innervation within the retinorecipient tectal volume. However, this doesn't show any variation and the trend remained the same across all the stages. The extent of innervation of the RGC tectal projections is not affected by the depletion of Fmn2. **(Figure 3.4)**

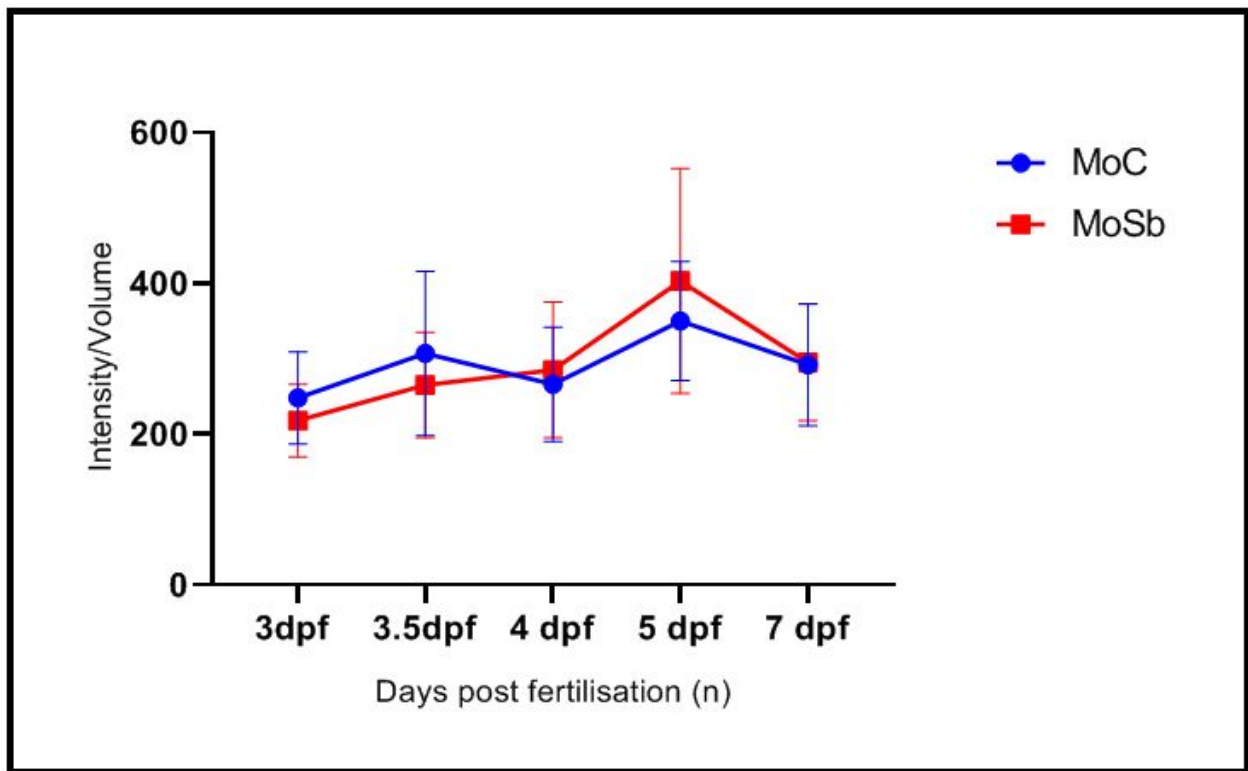


Figure 3.4: The intensity by volume of the projection of the RGC to the optic tectum in Fmn2 morphants and control zebrafish larvae remain unaffected.

The blue circle and red square represents control morpholino and splice blocking morpholino injected zebrafish larvae at 3dpf (n= 25,MoC ; 25,MoSb), 3.5dpf (n= 15,MoC ; 14,MoSb) 4dpf (n= 18,MoC ; 20,MoSb), 5dpf (n= 19,MoC ; 23,MoSb) and 7dpf(n=18,MoC ; 21,MoSb). Mann-Whitney non-parametric test.

3.2. Depletion of Fmn2 leads to a decrease in the size of the neuropil and optic tectum.

One possible reason for the reduction in the RGC tectal volume may be the reduction in the size of the optic tectum due to depletion of the Fmn2 expression. To answer this, we performed whole-mount immunostaining of the control and morphant zebrafish larvae. The stained larvae were mounted in a coverslip-bottom Petri plate and imaged using a confocal microscope. The maximum intensity projection (MIP) of confocal z-stacks of the whole-mount immunostained larval brain enabled us to visualise the neuropil which is the region within the red boundary, the SFGS and SO layers of the optic tectum represented by the anti-GFP bound region(white), SPV that is denoted by the DAPI-labelled (blue) area within the black dots and total optic tectum which is denoted by the area enclosed within the black dotted lines. The area of the neuropil, the projection of the *brn3c* positive RGCs, SPV and the optic tectum were quantified from the MIP. **(Figure 3.5)**

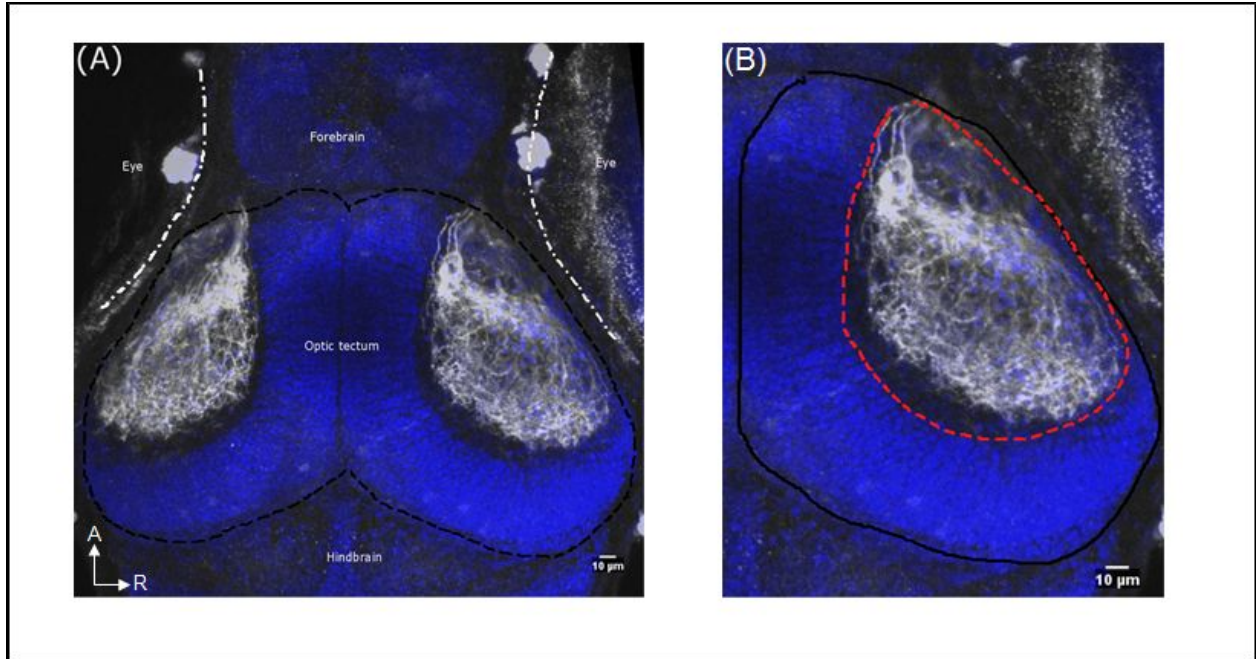


Figure 3.5: Whole-mount immunostaining of Tg(Brn3c:GAP43-GFP) to visualize different regions in the optic tectum.

(A) MIP of the dorsal view of the larval brain at 4dpf in Tg(Brn3c:GAP43-GFP). Brain morphology is visualized with the nuclear marker (DAPI) and the axonal projection of RGC (SFSGS and SO layer) by GFP antibody (white). The black dotted line represents the boundary of the optic tectum. **(B)** The boundary of the right optic tectum is marked by black line. The blue area enclosed represents the SPV and the red dotted line demarcates the neuropil.

There was a reduction in the area of the SPV, SFSGS and SO in the Fmn2 morphant zebrafish larvae compared to the control (**Figure 3.6 (A), (B), (D)**). The SFSGS and SO are two layers in the neuropil, we normalised the area of SFSGS and SO to that neuropil to measure the extent of innervation in the neuropil and observed that there was no significant (Mann Whitney, non-parametric t-test) difference. This concludes that the reduction is consistent in all the layers, and reduction in area is observed in the neuropil also (**Figure 3.6 (C)**).

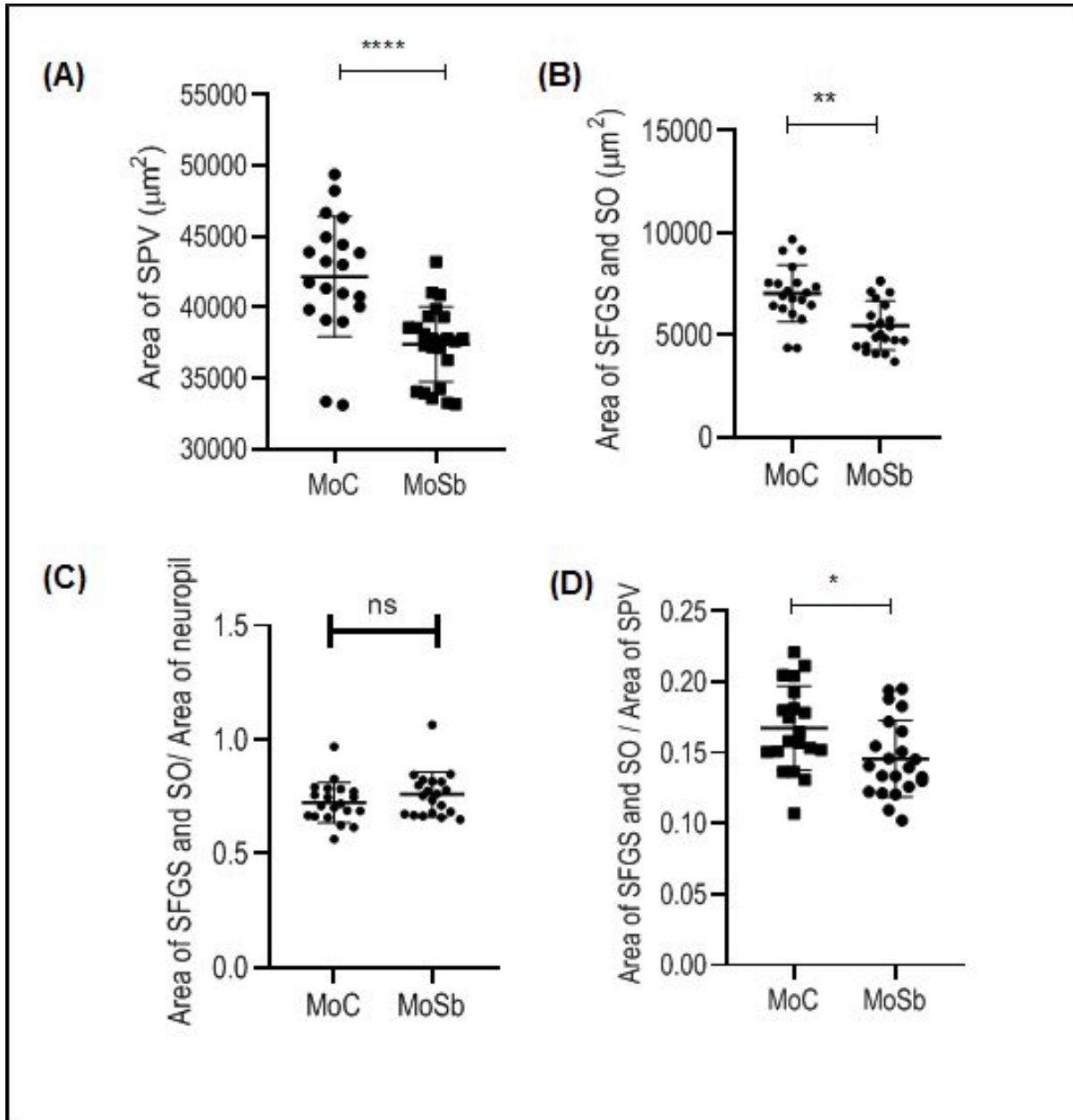


Figure 3.6: Decrease in the size of the neuropil and the optic tectum in the Fmn2 morphants at 4dpf.

There is a reduction in the area of the **(A) SPV** (**Figure 3.5(B)**) (n=20, MoC; 24;MoSB; p<0.0001), SFGS and SO (**Figure 3.2(B)**) (n=20,MoC; 22, MoSb; p=0/0011). The ratio of the area of SFGS and SO to that of the **(C) neuropil** (n=20, MoC; 20, MoSb) (**Figure 3.5(B)**) and to the **(D) SPV**(n=20, MoC; 22, MoSb; p=0.0162)

3.3. Fmn2 morphants may show deficits in visually guided behaviours

Zebrafish's survival is dependent on its ability to evaluate the sensory information and elicit the appropriate behavioural response. By 5dpf, zebrafish larvae are capable of performing a repertoire of sensorimotor behaviours, like a response to prey- or a predator-like response and other visual stimulations, change in visual field intensity. When an organism, prey or predator, approaches the zebrafish, the angle subtended by the organism on the eye of the zebrafish changes. Also, the speed of the approaching organism determines the behavioural response elicited by the zebrafish. Hence the response of larvae to a moving dot is either approach (prey-like stimulus) or avoidance (predator-like stimulus). The classifying objects based on the size is dependent on the processing of the information in the optic tectum (Barker and Baier, 2015) A large dot moving towards the zebrafish larvae elicits a response similar to that of a predator approaching and to avoid the predator, the zebrafish moves away from the predator. Freely swimming Fmn2 morphant and control zebrafish larvae were placed in a 24- well Petri plate and were placed above a screen. The zebrafish larvae that exhibited random movement in the absence of stimulus were used for further behavior experiments. This ensured the habituation of the larvae to the chamber. A Python-code was used to move a dot of 12-pixel size at a speed of 30 pixels per second on the screen. We looked at the response of the control and morphant larvae to a moving large dot stimulus on the screen below the chamber (**Figure 3.7**). Avoidance behaviors were markedly faster (always less than two frames at 60 Hz) and further characterized by swimming away from the direction of the dot's motion. A response was noted when the moving dot was within central 200° of the visual field of the zebrafish larvae.

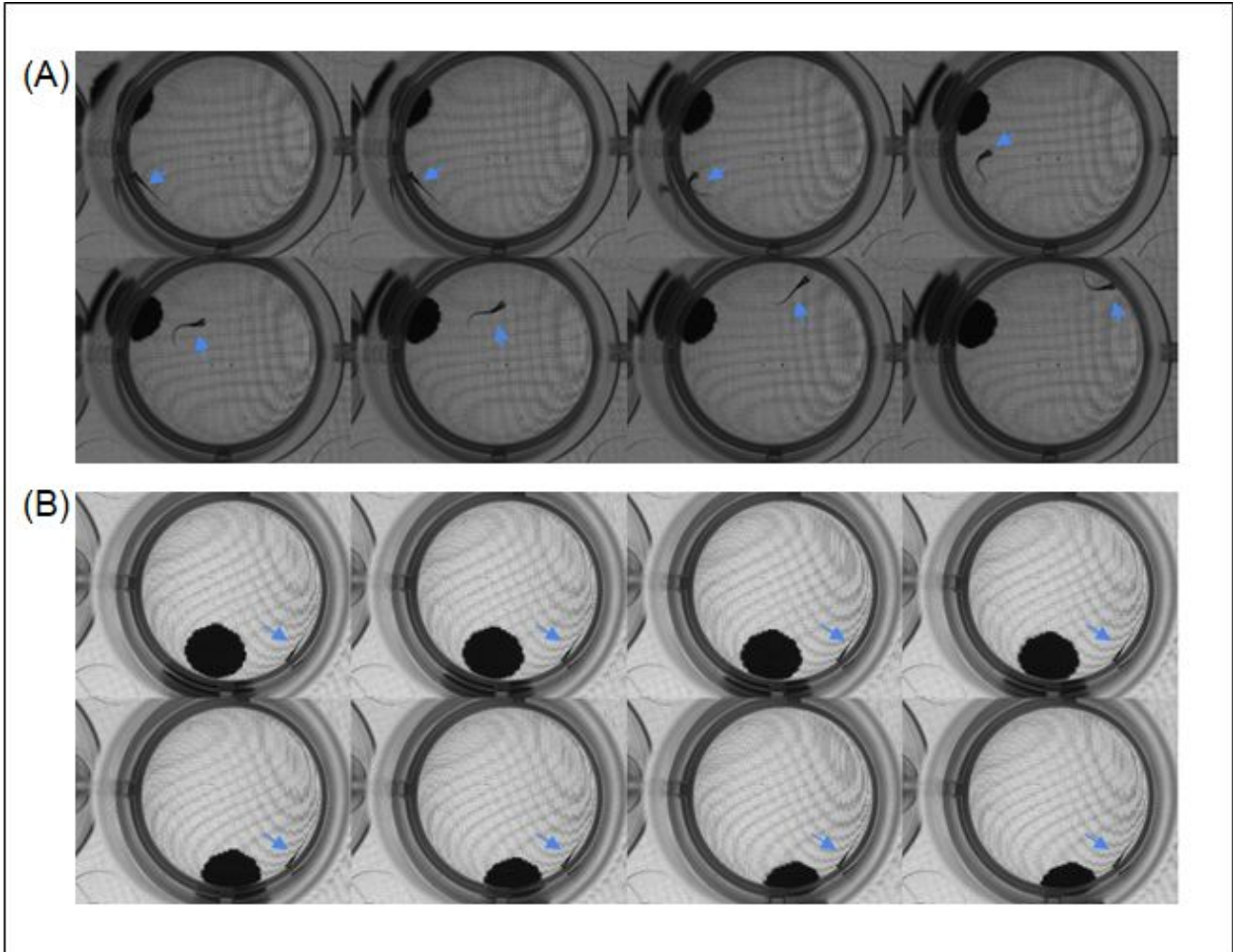


Figure 3.7: Response of the zebrafish larvae to a moving dot stimulus.

When presented by a moving large dot to a 5dpf Tg(Brn3c:GAP43-GFP), the response that was observed in the zebrafish larvae are (A) avoidance and (B) No response. Arrows point to the larvae. The blue arrows represent the position of the zebrafish larvae in one well of a 24-well plate.

The ratio of the number of responses of the zebrafish larva (**Figure 3.7**) to the total number of times the stimulus was within the visual field of the larva was quantified. Around 60% of the Fmn2 morphants tested showed a reduced response compared to the control. We found two populations within the MoSb zebrafish larvae, one which has a response index similar to that control and another one which has a defective

response. Thus concluding that depletion of Fmn2 may result in permanent deficits in the circuitry. (Figure 3.8)

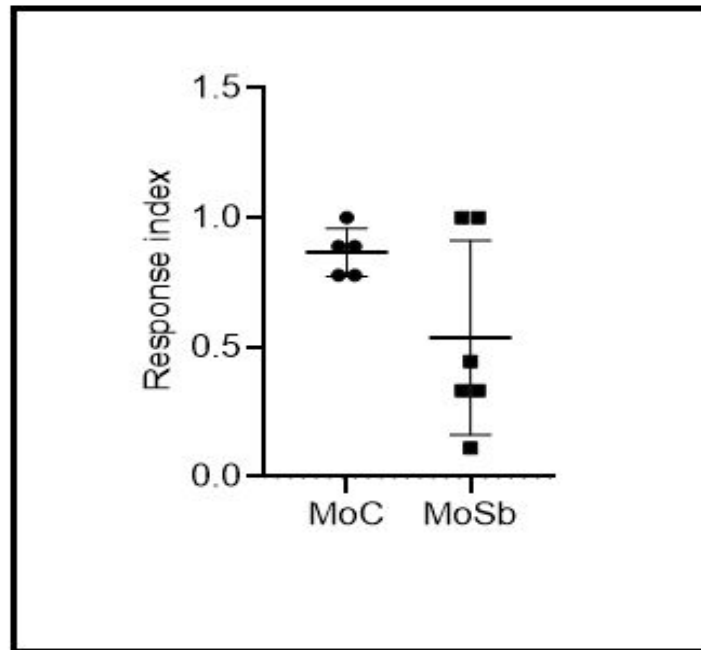


Figure 3.8: Response index of the Fmn2 morphants and control zebrafish larvae.

The graph represents the ratio of the number of times the larvae responded to the moving dot within its visual field to the number of times moving ball was within the visual field of the zebrafish larvae (n= 5, MoC; 6, MoSb)

3.4. Standardisation of Calcium imaging to visualise the activity in the optic tectum to a looming stimulus.

To visualise the activity of optic tectum to a visual stimulus in the Fmn2 knockdown zebrafish larvae, we standardised the setup and conditions for providing a looming stimulus. We used a transgenic zebrafish expressing the calcium indicator GCamp6f under the cytosolic *elavl3* promoter, which provides near-pan neuronal expression, *Tg(Elavl3:GCamp6f)* for the calcium imaging (Chen et al, 2013). We imaged the response of the optic tectum of a 3dpf transgenic zebrafish larvae to a looming stimulus, elicited by the gradual increase of a dot from radius; $r=0\text{cm}$ to $r=0.625\text{cm}$ on a screen below the chamber containing body-fixed larvae (**Figure 3.9**). The fluorescence changes in the cells over time was quantified (**Figure 3.10**).

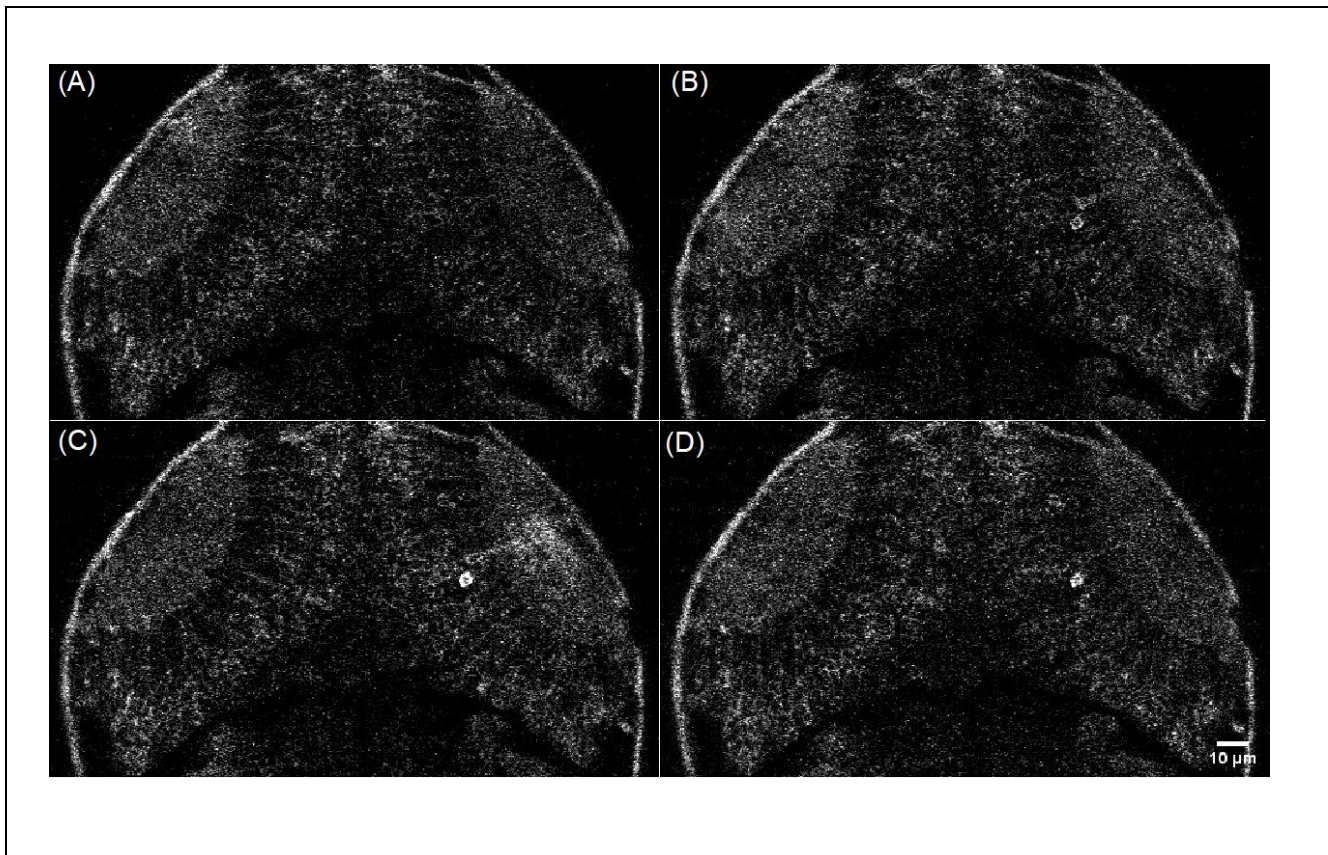


Figure 3.9: Calcium activity of a 3dpf zebrafish larvae to a looming stimulus.

The 3dpf zebrafish larvae were restrained in 2% agarose and the calcium activity in response to a looming stimulus was recorded. The images represent the calcium activity in the optic tectum (A) At $t=0$, (B) at $t= 2.5s$ (C) at $t= 5s$ and (D) at $t= 10s$ after the visual stimulus appears on the screen below the Petri plate containing the restrained larva.

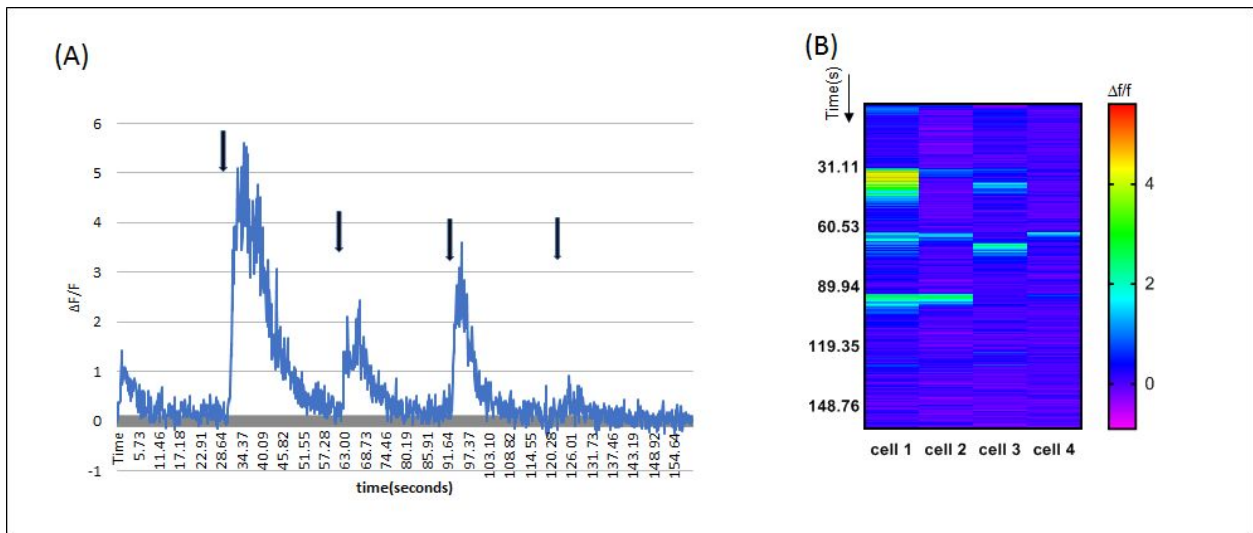


Figure 3.10: Standardization of the calcium response of a 3dpf zebrafish larvae to a looming visual stimulus.

(A) The activity of a single neuron over time in response to a black dot gradually increasing radius from 0cm to 0.625cm over a time of 10 seconds. The black arrows represent the start of the looming stimulus. **(B)** Heat-map of activity ($\Delta f/f$) of 4 different cells in the tectum in response to the looming stimulus is plotted

CHAPTER 4: DISCUSSION.

An organism is able to generate the appropriate behavioural response after processing the multimodal sensory information. The development of a precise neural circuit at the early stages plays an important role in eliciting a spectrum of such behaviour. The formation of a precise neural circuitry requires the growth cone to guide the axons of the neurons to their synaptic targets. This growth-cone mediated movement of the axon involves a dynamic remodelling of the growth cone cytoskeleton. There are many cytoskeletal remodelling proteins that are involved in this process and Fmn2 is one of the cytoskeletal remodelling proteins that was characterized in our lab.

In this thesis, I investigated the role of Fmn2 in the development of neural circuit development of zebrafish. Therefore the zebrafish retinotectal pathway which is a model system for axon guidance and mapping was studied. Fmn2 is an actin nucleator, F-actin bundler and elongator (Pfender et al., 2011). Fmn2 plays a novel role in the crosstalk between actin-microtubule, crucial for the cytoskeletal remodelling process (Kundu et al., 2020). Studies in chick spinal commissural neurons have shown that Fmn2 is necessary for axon outgrowth and guidance (Sahashrabudhe et al, 2016). Another study in the lab in chick spinal neurons has also shown that Fmn2 has a role in axonal branching (Das and Kundu). *In-situ* hybridization experiments in zebrafish larvae have shown the enrichment of Fmn2 mRNA in the RGCs of zebrafish larvae along with the CNS (Unpublished data, Dhriti Nagar). Fmn2 is a cytoskeletal remodelling protein which could be instrumental in dynamic processes of branching, arborization. Hence I looked for defects in the outgrowth and innervation in the retinotectal pathway.

We observed a reduction in the volume of the axonal projections innervating the optic tectum across different developmental time-points from 3dpf till 7dpf in the early stages of a zebrafish larvae. We looked at the arborization at 3dpf when the axonal projections of the RGC reach the tectum and begin to arborise till 5dpf. Then they undergo pruning

till 7dpf, so we looked at the arborization at 7dpf as a late stage of development. We have seen that for all the time points that we have looked at, the volume innervated by the RGC axon in optic tectum is lower in the Fmn2 morphants compared to the control larvae. From live imaging, Fmn2 morphant zebrafish showed a range of phenotypes for the reduced arborization in the optic tectum. Around 30% of the MoSb have the axonal projection of the RGCs reaching the optic tectum and starting to form arborize by 3.5dpf while the remaining 70% of MoSb have arborized extensively. This suggests that there is a difference in the degree of penetrance of the phenotype due to which the behavioural response of the larvae to any stimulus may also vary. The transgenic line that was used for the experiment was not strictly verified to be homozygous, thus it is possible that this contributes to the variability in both control and morphant larvae. Also, morpholino effectiveness reduces over time. Our lab determined that the knockdown efficiency is maximum at 2dpf and begins to show indications of dilution by 4dpf. As the development proceeds, the overall volume of the zebrafish embryo doesn't change but the number of nuclei increases. This leads to a decrease in the intranuclear morpholino concentration. This reduction in the morpholino concentration results in the effective splicing of mRNA and hence dilutes the effect of the splice-blocking morpholino. We can quantify the dilution in morpholino by RT-PCR as the insertion of an intron will show a change in the size of band in the RT-PCR product band on an agarose gel. However, we continue to see that the morpholino mediated knockdown persists during the development of RGCs and results in permanent deficits in the circuitry.

One of the possible reasons for the reduction in the volume innervated by the axonal projection of the RGCs to the optic tectum may be due to the decreased axonal branching. A study in the lab has also shown that Fmn2 is essential for the axonal branching process all along the axon (Das and Kundu). Another plausible reason is that the axons started to form arbors before reaching their topographic target location. This could lead to a decreased volume where the arborisation occurs. But the intensity which is the measure of arbors present within the volume also differ. Thus, we looked at the

intensity normalized to the volume of the axonal projection of RGC, which gives a measure of the extent of innervation. We haven't observed any difference in the extent of innervation in the optic tectum. **(Figure 3.4.)** Another plausible reason for the reduced volume occupied by the RGC arbors could be delayed axon outgrowth. We can confirm this by observing the RGC axon exiting the retina or crossing the midline in live imaging. Early born RGC project their axons and the axons of the late-born RGC follow that path laid by the pioneer ones. Retinoblastoma mutants(*rb1*) zebrafish larvae have shown the delayed onset of the early-born RGC, and a delayed axonal outgrowth and reduced tectal innervation were observed. They have observed increased apoptosis in the retina of the *rb1* mutant (Gyda et al., 2012).

An overall reduction in the size of the brain can also lead to a smaller volume of RGC axon tectal innervation. To answer this, we performed whole-mount immunostaining against GFP and DAPI and showed that there is a reduction in the size of the optic tectum in *Fmn2* morphants. We observed a decrease in the SPV and the SFGS and SO region of the optic tectum. In order to check if the extent of innervation in the neuropil is affected in *Fmn2* morphants, we normalised the area of SFGS and SO to that of neuropil and didn't observe any difference. This concluded that all layers of the neuropil undergo reduction. Also, the target tissue of the neuropil i.e. the SPV area showed a reduction. A study on zebrafish larvae has shown that retinal ganglion cell axon innervation regulates the size of the target tissue. They have seen a reduction in the size of the contralateral tectum when an eye is removed. (Rouse, 2015). There is a bidirectional relation between the regulation of the size of the target tissue and the innervation it receives. Thus led us to the conclusion that the reduction in the size of the optic tectum that we observe is due to the reduction in the RGC arbors and vice versa. The live imaging experiment and the whole-mount immunostaining together confirm that there is an overall reduction in the optic tectum including the neuropil area.

Interwired neural circuits work together to elicit the appropriate behaviour. To understand the implication of this phenotype in the functioning of the circuit and the ability to exhibit a behaviour, we looked at how the Fmn2 morphant responds to a moving dot stimulus. Around 60% of the response index in MoSb is below 0.5 (The larvae didn't respond to the moving dot for more than 4 times). The anatomical defects seen in the MoSb are not the same in all larvae (Figure 3.2). Due to the penetrance in this phenotype, we observed that there is variability in response of MoSb. Some Fmn2 morphants responded very similarly to the control zebrafish larvae, but there was a subset of the larvae which responded to the dot very poorly. But increasing the number of subjects will help to clearly overcome this issue. The deficit in the behaviour result is due to the cumulative effect of the knockdown of Fmn2 in the zebrafish larvae. Hence, it is important to see how Fmn2 depletion affects the functioning of the optic tectum.

There can be defects in the development of several other downstream circuits in the visual pathway. To improve our understanding of how these cytoskeletal defects have an effect on the functioning of the optic tectum, we standardized a calcium imaging setup and looked at the calcium activity of the neurons in the SPV to a looming visual stimulus. We observed a peak in the activity when the stimulus was presented. But we have seen a decrease in the peak with continuous trials. This might be due to less inter-trial intervals as some of the channels might be still in the refractory period.

Our observations point out that Fmn2 is important in RGC connectivity. We haven't looked at the exact mechanism involved in the process. This result helps to complement studies in our lab which were early done in cultured neurons in a living vertebrate model. We have laid out the foundation for future experiments so as to understand the role of Fmn2 in the functional aspects of the circuit.

4.1. Future directions

In order to observe how the arborization of each neuron is affected, we can perform sparse labelling of neurons using an appropriate plasmid. Injecting plasmid Brn3c:mGFP to Fmn2 morphant or mutant zebrafish larvae at the single-cell stage enable us to trace the development of a single RGC axon. Hence, allow us to understand the branching pattern of the RGC axon in the Fmn2 morphant. Looking at the arborisation at 34-36hpf, when the optic tectum is supposed to cross the midline will help us to understand if there is a delay in the axonal guidance of the axonal projection of the RGCs to the tectum.

Further, whole-mount staining using acridine orange or other apoptosis markers like caspase-3 will help us narrow down the possible reasons responsible for the observed defects.

Our lab has found that there are path-finding defects in the intertectal commissure neurons in the zebrafish larvae in Fmn2 morphants. The intertectal neurons connect the two tectal hemispheres and are involved in the integration of binocular visual inputs to elicit a prey capture response. It was shown that zebrafish larvae cannot initiate the capture swim in case of ablation in the intertectal neurons (Gebhardt et al, 2019). To observe the implication of the defect in axon-pathfinding of the intertectal commissure, in the visually evoked prey-capture response we can perform a prey consumption assay. The calcium imaging that is standardised can be used to observe the functional defects in the optic tectum due to the path-finding defects in the intertectal commissure. Enucleation of a single eye in the zebrafish larvae ensures that the tectum receives sensory information from one eye only. The activity of the tectum attached to the enucleated eye is dependent on the functioning of the intertectal commissure. Observing the activity of the tectum in Fmn2 morphant and control enable us to decipher whether depletion in Fmn2 compromises the functioning of the optic tectum in zebrafish.

REFERENCES

1. Agís-Balboa, R., Pinheiro, P., Rebola, N., Kerimoglu, C., Benito, E., Gertig, M., Bahari-Javan, S., Jain, G., Burkhardt, S., and Delalle, I. et al. (2017). Formin 2 links neuropsychiatric phenotypes at a young age to an increased risk for dementia. *The EMBO Journal* 36, 2815-2828.
2. Amores, A., Catchen, J., Ferrara, A., Fontenot, Q., and Postlethwait, J. (2011). Genome Evolution and Meiotic Maps by Massively Parallel DNA Sequencing: Spotted Gar, an Outgroup for the Teleost Genome Duplication. *Genetics* 188, 799-808.
3. Arimura, N., and Kaibuchi, K. (2007). Neuronal polarity: from extracellular signals to intracellular mechanisms. *Nature Reviews Neuroscience* 8, 194-205.
4. Baier, H., and Scott, E. (2009). Genetic and optical targeting of neural circuits and behaviour—zebrafish in the spotlight. *Current Opinion In Neurobiology* 19, 553-560.
5. Barker, A., and Baier, H. (2015). Sensorimotor Decision Making in the Zebrafish Tectum. *Current Biology* 25, 2804-2814.
6. Burrill, J., and Easter, S. (1994). Development of the retinofugal projections in the embryonic and larval zebrafish (*Brachydanio rerio*). *The Journal Of Comparative Neurology* 346, 583-600.
7. Cajal, S. R. (1890). Notas anatómicas I. Sobre la aparición de las expansiones celulares en la médula embrionaria. *Gac. Sanit. Barc.* 12, 413–419
8. Chao, D., Ma, L., and Shen, K. (2009). Transient cell-cell interactions in neural circuit formation. *Nature Reviews Neuroscience* 10, 262-271.

9. Chen W, Fischer A (2010) Altered histone acetylation is associated with age-dependent memory impairment in mice. *Science* 328: 753–756
10. Chen, T., Wardill, T., Sun, Y., Pulver, S., Renninger, S., Baohan, A., Schreiter, E., Kerr, R., Orger, M., and Jayaraman, V. et al. (2013). Ultrasensitive fluorescent proteins for imaging neuronal activity. *Nature* 499, 295-300.
11. Colwill, R., and Creton, R. (2011). Imaging escape and avoidance behaviour in zebrafish larvae. *Reviews In The Neurosciences* 22.
12. Das, S., and Kundu, T. Role of FMN2 in Axonal Branching. Indian Institute of Science Education and Research.
13. Davidson, A. E., Balciunas, D., Mohn, D., Shaffer, J., Hermanson, S., Sivasubbu, S., Cliff, M. P., Hackett, P. B., and Ekker, S. C. (2003). Efficient gene delivery and gene expression in zebrafish using the Sleeping Beauty transposon. *Dev. Biol.* 263, 191–202.
14. Del Bene F., Wyart C., Robles E., Tran A., Looger L., Scott E. K., et al. (2010). Filtering of visual information in the tectum by an identified neural circuit. *Science* 330 669–673
15. Dent, E., Gupton, S., and Gertler, F. (2010). The Growth Cone Cytoskeleton in Axon Outgrowth and Guidance. *Cold Spring Harbor Perspectives In Biology* 3, a001800-a001800.
16. Dent, E., Merriam, E., and Hu, X. (2011). The dynamic cytoskeleton: the backbone of dendritic spine plasticity. *Current Opinion In Neurobiology* 21, 175-181.
17. Dotti, C., Sullivan, C., and Banker, G. (1988). The establishment of polarity by hippocampal neurons in culture. *The Journal Of Neuroscience* 8, 1454-1468.
18. Erskine, L., and Herrera, E. (2007). The retinal ganglion cell axon's journey: Insights into molecular mechanisms of axon guidance. *Developmental Biology* 308, 1-14.

19. Gahtan, E. (2005). Visual Prey Capture in Larval Zebrafish Is Controlled by Identified Reticulospinal Neurons Downstream of the Tectum. *Journal Of Neuroscience* 25, 9294-9303.
20. Gebhardt, C., Auer, T., Henriques, P., Rajan, G., Duroure, K., Bianco, I., and Del Bene, F. (2019). An interhemispheric neural circuit allowing binocular integration in the optic tectum. *Nature Communications* 10.
21. Geraldo, S., and Gordon-Weeks, P. (2009). Cytoskeletal dynamics in growth-cone steering. *Journal Of Cell Science* 122, 3595-3604.
22. Gonzalo G. De Polavieja., and German Sumbre. (2014). The world according to zebrafish: How neural circuits generate behaviour (Frontiers Media SA).
23. Gräff, J. (2017). Forming a link between PTSD and AD. *The EMBO Journal* 36, 2809-2811.
24. Gyda, M., Wolman, M., Lorent, K., and Granato, M. (2012). The Tumor Suppressor Gene Retinoblastoma-1 Is Required for Retinotectal Development and Visual Function in Zebrafish. *Plos Genetics* 8, e1003106.
25. Higgs, H. (2005). Formin proteins: a domain-based approach. *Trends In Biochemical Sciences* 30, 342-353.
26. Hu, M., and Easter, S. (1999). Retinal Neurogenesis: The Formation of the Initial Central Patch of Postmitotic Cells. *Developmental Biology* 207, 309-321.
27. Hutson, L., and Chien, C. (2002). Wiring the zebrafish: axon guidance and synaptogenesis. *Current Opinion In Neurobiology* 12, 87-92.
28. Kawakami, K. (2004). Transgenesis and gene trap methods in zebrafish by using the Tol2 transposable element. *Methods Cell Biol.* 77, 201–222.
29. Kawakami, K., Shima, A., and Kawakami, N. (2000). Identification of a functional transposase of the Tol2 element, an Ac-like element from the Japanese medaka fish, and its transposition in the zebrafish germ lineage. *Proc. Natl. Acad. Sci. U.S.A.* 97, 11403–11408
30. Kevenaar, J., and Hoogenraad, C. (2015). The axonal cytoskeleton: from organization to function. *Frontiers In Molecular Neuroscience* 8.

31. Kita, E., Scott, E., and Goodhill, G. (2015). Topographic wiring of the retinotectal connection in zebrafish. *Developmental Neurobiology* 75, 542-556.
32. Kubo, F., Hablitzel, B., Dal Maschio, M., Driever, W., Baier, H., and Arrenberg, A. (2014). Functional Architecture of an Optic Flow-Responsive Area that Drives Horizontal Eye Movements in Zebrafish. *Neuron* 81, 1344-1359.
33. Kundu, T., Dutta, P., Nagar, D., Maiti, S., and Ghose, A. (2020). Coupling of dynamic microtubules to F-actin by Fmn2 regulates chemotaxis of neuronal growth cones.
34. Lasser, M., Tiber, J., and Lowery, L. (2018). The Role of the Microtubule Cytoskeleton in Neurodevelopmental Disorders. *Frontiers In Cellular Neuroscience* 12.
35. Law R, Dixon-Salazar T, Jerber J, Cai N, Abbasi AA, Zaki MS, Mittal K, Gabriel SB, Rafiq MA, Khan V, Nguyen M, Ali G, Copeland B, Scott E, Vasli N, Mikhailov A, Khan MN, Andrade DM, Ayaz M, Ansar M *et al* (2014) Biallelic truncating mutations in FMN2, encoding the actin-regulatory protein Formin 2, cause nonsyndromic autosomal-recessive intellectual disability. *Am J Human Genet* 95: 721–728
36. Leader, B., and Leder, P. (2000). Formin-2, a novel formin homology protein of the cappuccino subfamily, is highly expressed in the developing and adult central nervous system. *Mechanisms Of Development* 93, 221-231.
37. Lowery, L., and Vactor, D. (2009). The trip of the tip: understanding the growth cone machinery. *Nature Reviews Molecular Cell Biology* 10, 332-343.
38. Meek, J., and Schellart, N. (1978). A Golgi study of goldfish optic tectum. *The Journal Of Comparative Neurology* 182, 89-121.
39. Menon, S., and Gupton, S. (2016). Building Blocks of Functioning Brain: Cytoskeletal Dynamics in Neuronal Development. *International Review Of Cell And Molecular Biology* 183-245.
40. Nevin, L., Robles, E., Baier, H., and Scott, E. (2010). Focusing on optic tectum circuitry through the lens of genetics. *BMC Biology* 8, 126.

41. O'Donnell, M., Chance, R., and Bashaw, G. (2009). Axon Growth and Guidance: Receptor Regulation and Signal Transduction. *Annual Review Of Neuroscience* 32, 383-412.
42. Orger, M., and de Polavieja, G. (2017). Zebrafish Behavior: Opportunities and Challenges. *Annual Review Of Neuroscience* 40, 125-147.
43. Robles, E., Filosa, A., and Baier, H. (2013). Precise Lamination of Retinal Axons Generates Multiple Parallel Input Pathways in the Tectum. *Journal Of Neuroscience* 33, 5027-5039.
44. Robles, E., Laurell, E., and Baier, H. (2014). The Retinal Projectome Reveals Brain-Area-Specific Visual Representations Generated by Ganglion Cell Diversity. *Current Biology* 24, 2085-2096.
45. Roeser, T., and Baier, H. (2003). Visuomotor Behaviour in Larval Zebrafish after GFP-Guided Laser Ablation of the Optic Tectum. *The Journal Of Neuroscience* 23, 3726-3734.
46. Rouse, H., 2015. *Retinotectal Projections Influence Optic Tectum Growth In Zebrafish*. PhD. Department of Cell and Developmental Biology, University College London.
47. Sahasrabudhe, A., Ghate, K., Mutalik, S., Jacob, A., and Ghose, A. (2015). Formin 2 regulates the stabilization of filopodial tip adhesions in growth cones and affects neuronal outgrowth and pathfinding in vivo. *Development* 143, 449-460.
48. Schelski, M., and Bradke, F. (2017). Neuronal polarization: From spatiotemporal signalling to cytoskeletal dynamics. *Molecular And Cellular Neuroscience* 84, 11-28.
49. Schumacher, N., Borawski, J., Leberfinger, C., Gessler, M., and Kerkhoff, E. (2004). Overlapping expression pattern of the actin organizers Spir-1 and formin-2 in the developing mouse nervous system and the adult brain. *Gene Expression Patterns* 4, 249-255.

50. Scott, E. (2009). The cellular architecture of the larval zebrafish tectum, as revealed by Gal4 enhancer trap lines. *Frontiers In Neural Circuits* 3.
51. Semmelhack, J., Donovan, J., Thiele, T., Kuehn, E., Laurell, E., and Baier, H. (2014). A dedicated visual pathway for prey detection in larval zebrafish. *Elife* 3.
52. Shen, K., and Cowan, C. (2010). Guidance Molecules in Synapse Formation and Plasticity. *Cold Spring Harbor Perspectives In Biology* 2, a001842-a001842.
53. Stuermer, C. (1988). Trajectories of regenerating retinal axons in the goldfish tectum: II. Exploratory branches and growth cones on axons at early regeneration stages. *The Journal Of Comparative Neurology* 267, 69-91.
54. Tau, G., and Peterson, B. (2009). Normal Development of Brain Circuits. *Neuropsychopharmacology* 35, 147-168.
55. Temizer, I., Donovan, J., Baier, H., and Semmelhack, J. (2015). A Visual Pathway for Looming-Evoked Escape in Larval Zebrafish. *Current Biology* 25, 1823-1834.
56. Tessier-Lavigne, M., and Goodman, C. (1996). The Molecular Biology of Axon Guidance. *Science* 274, 1123-1133.
57. Thermes, V., Grabher, C., Ristoratore, F., Bourrat, F., Choulika, A., Wittbrodt, J., and Joly, J. S. (2002). I-SceI meganuclease mediates highly efficient transgenesis in fish. *Mech. Dev.* 118, 91–98.
58. Weiner, J., Jontes, J., and Burgess, R. (2013). Introduction to mechanisms of neural circuit formation. *Frontiers In Molecular Neuroscience*
59. Winkle, C., and Gupton, S. (2016). Membrane Trafficking in Neuronal Development: Ins and Outs of Neural Connectivity. *International Review Of Cell And Molecular Biology* 247-280
60. Xiao, T. (2005). A GFP-based genetic screen reveals mutations that disrupt the architecture of the zebrafish retinotectal projection. *Development* 132, 2955-2967.